7-21-2008

BPSK system analysis using MEMS filters

David Ho

David Ho
_____
Candidate

Electrical and Computer Engineering (ECE)
_____
Department

This thesis is approved, and it is acceptable in quality
and form for publication on microfilm:

Approved by the Thesis Committee:

_____, Chairperson

_____

_____

_____

_____

Accepted:

_____
Dean, Graduate School

_____
Date

BPSK System Analysis Using MEMS Filters

by

David Ho

BS., Electronics Engineering Technology, DeVry University, 2002

THESIS

Submitted in Partial Fulfillment of the
Requirements for the Degree of

**Master of Science
Electrical Engineering**

The University of New Mexico
Albuquerque, New Mexico

May, 2008

Dedication

In memory of Mary, Jeremiah, and our unborn children. To my family, especially my wife, Sarah, for all of her love and support. To Summer, Faith and Abigail, God has big plans for your life; work hard to glorify His name!

Acknowledgments

I would like to thank God, for the blessings of knowledge, perseverance, and patience. He deserves credit for all I do, because what I see as an impossible task, is made possible through Him. I would also like to say thanks to my wife, Sarah, for her constant love and support. Also, to my daughters, Summer, Faith, and Abigail for giving me their continuous patience over the years. A special thanks goes to my Life Group. Your prayers have not been wasted and I thank you for your continuous support.

I would also like to thank my co-workers and management at Sandia National Laboratories for supporting this effort. The management was supportive in my decision to further my education and to all my co-workers, especially Nick Bikhazi, Troy Olsson, and David Heine. You patiently and clearly explained answers to all my questions.

Finally, I would like to thank my parents for loving me and supporting me throughout this process. You've given me the foundation I needed to complete this task.

BPSK System Analysis Using MEMS Filters

by

David Ho

ABSTRACT OF THESIS

Submitted in Partial Fulfillment of the
Requirements for the Degree of

**Master of Science
Electrical Engineering**

The University of New Mexico
Albuquerque, New Mexico

May, 2008

BPSK System Analysis Using MEMS Filters

by

David Ho

BS., Electronics Engineering Technology, DeVry University, 2002
MS., Electrical Engineering, University of New Mexico, 2008

Abstract

For some military applications, there exists a need for small custom radios. These radios need to be able to survive extreme environments and transmit the necessary data. This can be achieved by using banks of micromechanical filters. These small filters are post-CMOS compatible, allowing hundreds of high-Q filters to be incorporated over a typical RF transceiver die. Selection of these filters allows the band, channel, and bandwidth to be rapidly changed in operation. Having integrated Microelectromechanical Systems (MEMS) filters eliminates the need for off-chip components such as crystal references and Surface Acoustic Wave (SAW) filters. This allows for smaller, low power, high performance, shock hardened radios to be developed.

This thesis will examine the simulation and system analysis of MEMS filters. In past literature, there have been advances in transceiver architecture that have reduced the number of parts, but many of these approaches have sacrificed RF performance. The zero-IF and LOW-IF direct conversion sacrifices RF performance, but is good enough for normal applications. For specific military applications, this RF sacrifice is not

acceptable. This thesis will simulate a BPSK architecture to develop an understanding

that the post-CMOS filters can reliably be trusted upon in communication systems. The

initial system to be simulated will be a 5-channel MEMS filter. This thesis will also

present actual results of the 5-channel MEMS filter.

Contents

List of Figures

xiii

List of Tables

Chapter 1

Introduction

In today's society, we want things as small and as fast as possible when it comes to electronics. The cell phone, GPS units, and many other commercially available devices are continuously trying to take advantage of the advances in engineering to incorporate a product that has been miniaturized and utilizes low power. Let's take the cell phone as a prime example. A cell phone is more than just a few chips and a battery pack. Buried inside the cell phone is a communications system made up of many passive components. These filters, resonators, and duplexers help sort out all the radio frequencies to insure that you receive your calls and not someone else's. What would it be like to have no dropped calls and a smaller phone? The marketplace for cell phones, GPS units, and other consumer friendly devices has shifted the focus of research in the microwave and millimeter wave area towards consumer applications. The long-established defense-related applications still have a high need for these products too. Consequently, industry has been investigating and taking advantage of the Microelectromechanical Systems (MEMS) that have been developed.

Microelectromechanical Systems (MEMS) devices have been around in the electronic industry since the 1970s. These devices were used for pressure and temperature sensors, accelerometers, and other sensor devices [1]. Although, the actual acronym MEMS wasn't coined until the 1980s [2], MEMS encompasses all miniaturized devices. It wasn't until the 1980s and into the mid 1990s that MEMS devices could be used for Radio Frequency (RF) Microwave Applications. The mid 1990s to present day has seen the MEMS technology move from technology research to fabrication process development to commercialization of MEMS products. This area has gained such publicity and success in recent years that by 2003 there are over 130 companies pursuing different MEMS applications [3]. The MEMS based industry is a billion dollar industry in the United States and is expected to grow even more in the future.

1.1   RF MEMS Areas

The term RF MEMS "refers to the design and fabrication of MEMS for RF integrated circuits [4]." Traditional MEMS is divided into two classes, actuators and sensors [4], but the research of RF MEMS technology is broken down into four distinct areas. Those four areas of RF MEMS research are:

- RF MEMS switches, varactors, and inductors

- Micromachined transmission lines, high-Q resonators, filters and antennas

- FBAR (thin film bulk acoustic resonators) and filters

- RF micromechanical resonators and filters

1.1.1   RF MEMS Switches, Varactors, and Inductors

This area is considered a "mature technology" because it has been thoroughly demonstrated from Direct Current (DC) -120 GHz [1]. Common MEMS switch types are a thin metal cantilever, air bridge, diaphragm, or some other structure electrically configured in series or parallel with an RF transmission line and designed to open the line or shunt it to ground upon actuation of the MEMS. Such switches have displayed excellent RF characteristics, including low insertion loss values, high linearity, better isolation, and the potential for integration. Figure 1.1 shows an example of a RF MEMS switch that NASA has been investigating for their systems.   In all spacecrafts with communications systems, there is a possibility to implement some type of RF switching network. These communication systems usually suffer from high insertion loss and low isolation in solid-state switches [5]. MEMS switch development can help cure these problems compared to the regular pin-diodes and metal semiconductor field-effect transistors. NASA's extensive research has shown that the RF MEMS technology offers the necessary performance advantages over the existing solid-state switches that they currently use.   Other devices such as varactors and inductors can also benefit from MEMS manufacturing to produce smaller products with the same results as conventional semiconductor devices.
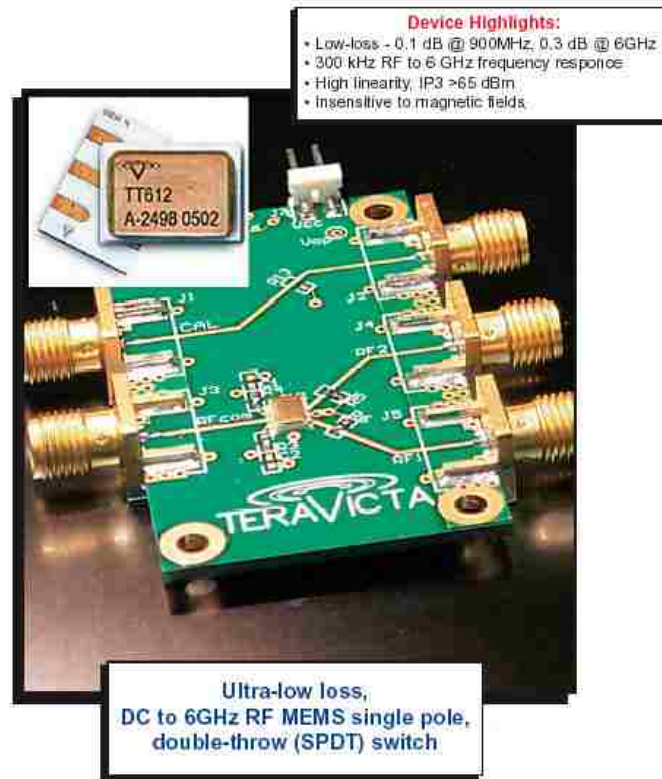
Figure 1.1 RF MEMS Switch [5].

1.1.2 Transmission Lines and Antennas

This area is usually good for frequencies of 12-200 GHz [1]. These types of MEMS devices are static and do not move [6]. The majority of MEMS devices that fall under this category are fabricated using silicon technologies such as Complimentary Metal Oxide Semiconductor (CMOS). They are able to use a process called wet etching to form transmission lines, inductors, capacitors, and couplers [4]. The way the MEMS are fabricated will be the discussion of Chapter 2. The MEMS antenna is important to

making the size of electronics smaller because many electronic devices are governed by antenna size. Figure 1.2 shows how a micromachined antenna is put together. The increased reliance of modern electronics on higher frequencies forces antenna size to become smaller and smaller, so fabrication of antennas is slowly transitioning to the use of micromachining procedures.
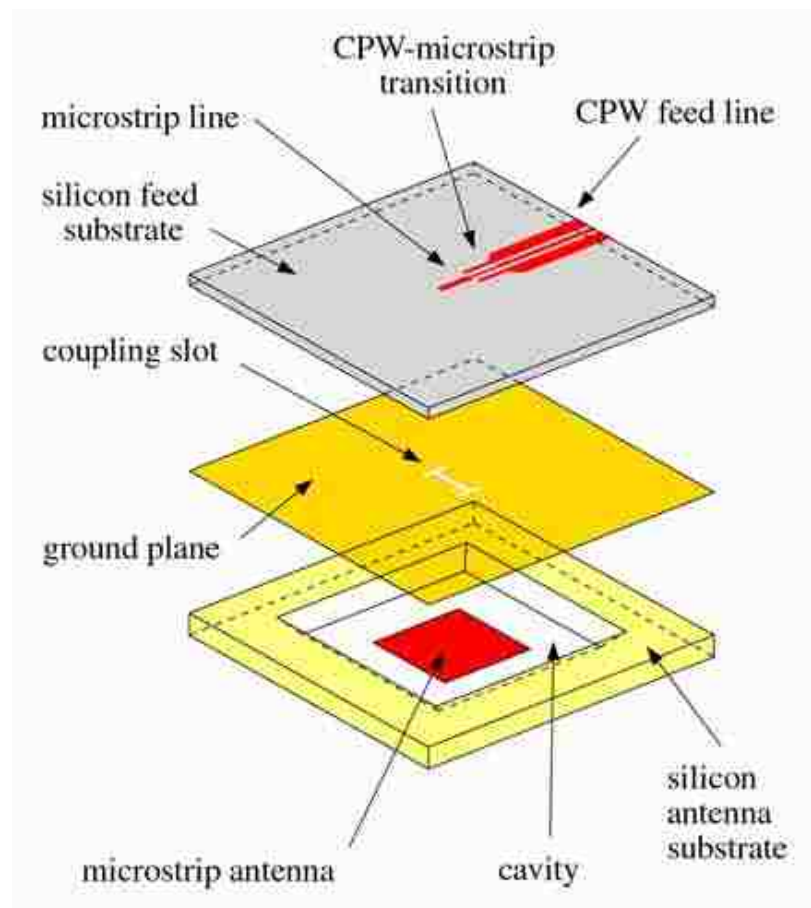
Figure 1.2 Synthesized low dielectric-constant antenna at 94 GHz [7].

1.1.3 FBAR (Thin Film Bulk Acoustic Resonators) and Filters

The FBAR technology is the most successful RF MEMS technology so far. It is fabricated using MEMS technology and they are able to produce many FBAR filters in a very small size. FBAR filters exploit acoustic vibrations in thin films and this has produced some very good results. They exhibit good performance up to 3 GHz and have a very high Q (>2000). This has resulted in the development of miniature low-loss filters for wireless applications [8]. The problem with FBAR filters is their center frequency is dependent upon the thickness of the thin film. Thus, multiple frequencies can not be fabricated on the same die and it is very costly to get two filters exactly alike from different dies. Figure 1.3 shows a California Short Grain of rice with four FBAR filters. FBAR filters are designed for cell phone applications, primarily by Avago (formerly Agilent). Integrating FBARS of different operating frequencies is very difficult because the frequency of operation is dependent upon Aluminum Nitride (AlN) or Zinc Oxide (ZnO) thickness. Using lithography it would be simplest (highest probability for success) to attempt to obtain one layer thickness upon a wafer. To produce any substantial number of FBAR filters would cost a lot of money. It is desirable, using RF MEMS filters, to put multiple oscillators/filters upon a single chip to mitigate size and power.
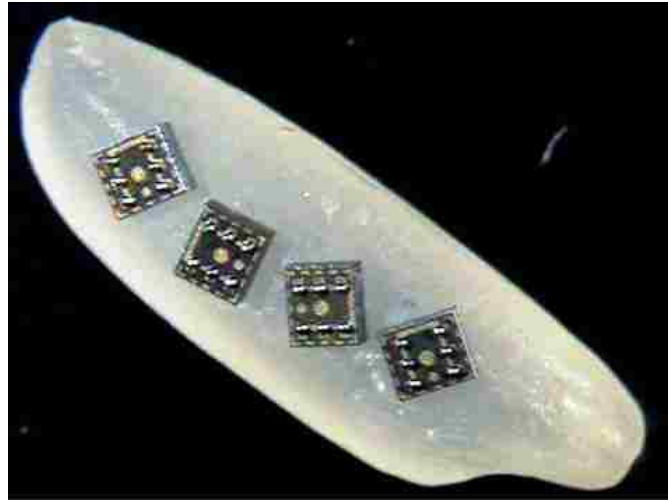
Figure 1.3 Agilent FBAR's on a Grain of Rice (Courtesy of Agilent).

1.1.4 RF Microelectromechanical Resonators and Filters

These use the mechanical vibrations of the device to achieve high-Q resonance. The Q is a measure of quality, how well a resonator or filter retains its energy. SiTime's products, technical papers from Discera Corp., and other literature have proven that MEMS resonators are capable of Q factors greater than 500,000 [9]. In the cell phone example, the designers want the filter's frequency selectivity to be as high as possible. The higher a filter's Q, the greater its selectivity in isolating frequencies. Integrated circuit filters have a Q of about 20, compared with SAW devices, in which the Q rises to 2,000. And MEMS-based filters are at least five times better than SAW filters. The MEMS filters are in a research phase of development and have yet to be introduced into system implementation [10].

Figure 1.4 shows a photo of dual mode Aluminum Nitride (AlN) band pass filter at 108.4 MHz which was developed at Sandia National Laboratories. This filter was made out of AlN and fabricated using a post-CMOS compatible process.

Input Electrode

280 µm

Output Electrode
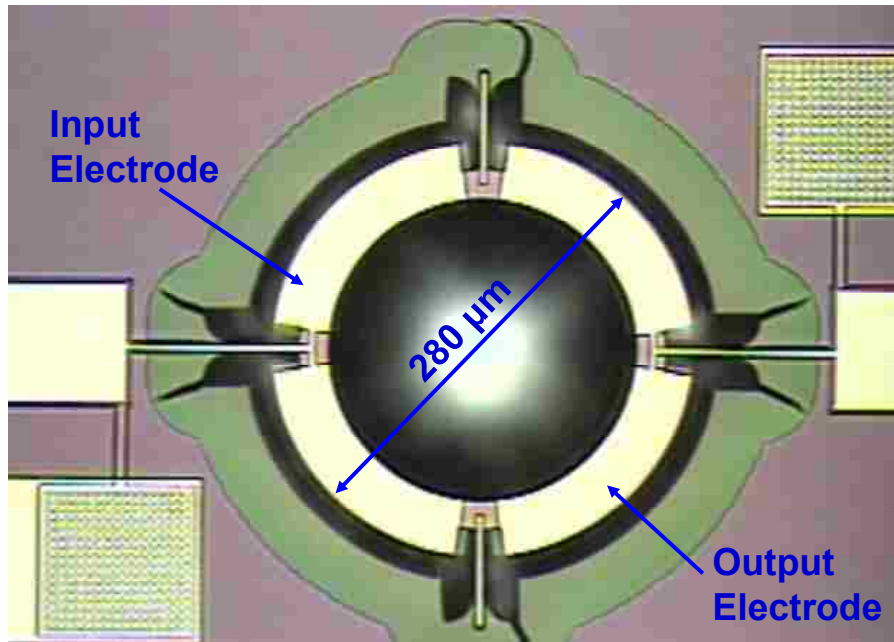
Figure 1.4 Dual Mode Aluminum Nitride Band Pass Filter.

This technology is what is being developed by Sandia National Laboratories and the fabricated MEMS filter will be the baseline of this thesis. The MEMS filter will be explained in more detail on its fabrication process and its operating requirements. It will be implemented into a BPSK architecture and the results will be presented.

1.2   Organization of Thesis

Many communications applications, each with their own performance requirements, could benefit from their own custom type radio. The primary application of interest in this thesis is the development of Radio Frequency Microelectromechanical (RF MEMS) Filters. The development of the RF MEMS filter is in process at Sandia National Laboratories. This is the first type of device of its kind in industry and this thesis will examine the performance of these devices through simulations and actual measured results.

The remainder of the thesis is organized as follows: Chapter 2 contains a background of MEMS devices that are being created in industry and at Sandia National Laboratories. It will discuss some of the processes in which RF MEMS devices are being created. In Chapter 3, the RF MEMS devices that were created is introduced and simulated in a MATLAB model. Chapter 3 includes a performance analysis based on MATLAB simulation results of a 5-channel MEMS filter. Chapter 4 extends the performance analysis of the MEMS filter into a BPSK system. Chapter 4 extends that performance analysis by presenting an analysis based on results gathered from simulating the system in MATLAB and performing an actual test using a real device. Chapter 5 concludes this thesis and provides suggestions for future work.

Chapter 2

Background

MEMS technology is a result of a long history of technological development that started way back when semiconductors were discovered. MEMS products were initially limited to sensors. Throughout the years, it has developed into a technology that impacts our daily life. An example of how it is used in our daily life is the automobile [11]. Many of the tiny sensors that are on the automobile use some type of MEMS technology. MEMS integrates the accelerometers and electronics onto a single silicon chip that is used to control the air bag deployment systems. Another example is the advancement of High Definition Television (HDTV). The digital light processors (DLPs) in projectors and television sets are also in the broad range of categories which MEMS is affecting. These two simple examples are just a small portion of how MEMS impacts our society. MEMS devices are also in the medical market, robotics, and space applications. MEMS have grown into an industry which affects our economy.

This chapter will explore the process used to develop an Integrated Circuit (IC). This same process is then altered slightly to develop a MEMS device. Sandia National Laboratories has also altered their process to develop a post-CMOS compatible MEMS

device. This process will be introduced in this Chapter and this device will be the device that will be used for simulations and for actual measurements when integrated into a BPSK receiver.

2.1   IC Fabrication

Integrated circuits are "the physical realization of a number of electrical elements inseparably associated on or within a continuous body of semiconductor material to perform the functions of a circuit" (Electronic Industries Alliance (EIA) definition [12]). Most everyday electrical devices are made up of several IC's. These IC's are developed with semiconductor materials. Semiconductors are a group of materials that have electrical conductivities intermediate between those of metals and insulators. Silicon is used for the majority of semiconductor devices. These devices are constructed out of the semiconductor fabrication processes that have made technological companies such as Intel, ON Semiconductor, and Samsung prosper over the past decades. These companies have expanded the economy and with the high demand to continue researching this area, it is expected to grow even more. So a lot of time and money has been invested into this process. This process takes a wafer and develops semiconductor integrated circuits in many processing steps. These steps can usually be grouped into a front end and back end processing technique. The front end processing is generally where the IC is created and

11

processed on the wafer, while the back end processing is the test, assembly, and packaging of the IC.

2.2   Front End Processing

The following process describes most of the key processes in developing IC's, but it is much more extensive than will be mentioned here.   Front end processing is the wafer development and processing.   A wafer of silicon is fabricated, sliced and polished from an ingot of silicon.   The thickness at which the silicon is sliced and polished is dependent upon the application.   The performance characteristics of all semiconductor devices are sensitive to the cleanliness in processing.   In order to create the best IC possible, there are many substrate cleaning procedures that are done at initiation of the process and throughout various steps in the process.   Any type of contaminant defects will destroy the operation of an IC, so it is crucial that the silicon is ultra-pure. In order to create the best possible quality of silicon, a pure layer of silicon is grown on the raw wafer through an epitaxial growth process. This layer is known as the epi-layer.   All IC processes involve a number of thin films.   These films are formed through various techniques, but they are integral to the structure of the particular IC.   The next step is to design a mask.   This mask is like a photographic negative, which is called lithography.   It defines the pattern that forms the physical elements of the integrated circuit.   The wafer is coated with a resist material, and then baked to make it harder.   The pattern is then exposed over the

wafer. The resist is then developed to create the pattern on the wafer. Now that the wafer is fully coated in an oxide, we need to pattern that oxide with a process called etching. There are two categories of etching, wet and dry. This process removes the oxide where there is no pattern. This also removes the mask that was used to develop the pattern.

As mentioned previously, the silicon process needs to be very clean, so the etching step needs to be done with great care in order to completely remove the resist material. The electronic and optical properties of semiconductor materials are strongly affected by impurities, which may be added in precisely controlled amounts. This process of controlled addition of impurities is called doping. By selectively patterning the stack of thin film materials with the appropriate set of masks, we can create the IC that we would like. The final step in front end processing is to add some passivation oxide layers to protect the surface of the wafers during back end processing.

2.3   Back End Processing

Back end processing is the testing, assembly, and packaging of the individual IC's. Once the front end processing is complete, the wafers go through extensive testing to verify the functionality of the IC's. There are many special tools to verify functionality of the IC's. These testing processes and tools will not be discussed in this thesis. Once the wafer has been thoroughly tested, feedback is given to the fabrication process. This gives them a

yield of good chips/bad chips. This will help them to improve the process for future wafers. The wafer is then carefully dissected into individual chips and each IC is tested for final functionality. The final IC is packaged and then it is sold to the customers for integration into whatever design they need it for. As stated previously, the process is much more detailed than what was mentioned here, but a general idea has been presented.

2.4   MEMS Fabrication

MEMS devices are fabricated using microfabrication technology similar to that used for integrated circuits. In most cases MEMS exist on a common silicon substrate; however, MEMS can be combined as discrete microcomponents in a single package.   While MEMS electronics are fabricated using IC process materials and process sequences, many times the micromechanical components, sensors, and actuators are fabricated using compatible "micromachining" processes that deposit new layers or selectively etch away parts of the silicon wafer to form the mechanical and electromechanical devices [12]. Even though MEMS fabrication uses many of the materials and processes of IC fabrication, there are important distinctions between the two technologies. The number, sequence, type of deposition, removal, and patterning steps used to fabricate devices are different. There are also differences in the method of wafers, freeing of parts designed to move, packaging, and testing. It's not so much the process that is being used, but how the process is being used. There are three dominant MEMS fabrication technologies [3]:

14

- Sacrificial surface micromachining

- Bulk micromachining

- LIGA (Lithographic, Galvanoformung, Abformung)

2.4.1 Sacrificial Surface Micromachining

Sacrificial surface micromachining uses the same concept as IC fabrication. This technique uses deposition, patterning, and etching of materials upon a typical silicon substrate. Essentially, it is a deposition of layers on the silicon wafer's surface. The materials consist of alternating layers of a structural material and a sacrificial material. As each layer is deposited, it is patterned, leaving material only where it is desired. When the sacrificial material is removed, the complete mechanical device is left. The sacrificial material is removed at the end of the fabrication process using a selective etch process that will not damage the structural material. In this method, all the MEMS structures are built on top of the silicon wafer. MEMS devices that have complicated components, such as a cantilever beam, are built using this technique. A cantilever beam is built by depositing and structuring a sacrificial layer, which is then selectively removed at the locations where the future beams must be attached to the substrate. The structural layer is then deposited on top of the polymer and structured to define the beams. The last step is to remove the sacrificial layer by using a selective etch process. Surface micromachining promotes large arrays of devices because no assembly is required.

2.4.2 Bulk Micromachining

Bulk micromachining is primarily a silicon based technology that utilizes wet or dry etch processes. It uses techniques such as etch stops and material selectivity to make useful devices. This type of machining is different from surface machining because it defines structures by selectively etching inside a substrate (typically silicon).

Bulk micromachining begins with a silicon wafer and it selectively etches into the substrate. It uses photolithography to create the pattern into the substrate. Once the pattern is created, wet or dry etching occurs. Most commonly this type of process uses wet etching, because wet etching takes advantage of how the silicon crystal structure is bonded together. The wafer is photo patterned, and then the wafer is dipped into a liquid etchant to eat away at the unwanted silicon. This makes the process simple and very inexpensive when making mass quantities. This type of processing is usually what creates most of the pressure sensors that we have today. Ultimately, sacrificial surface micromachining creates structures on top of a substrate, while bulk micromachining produces structures inside a substrate.

2.4.3 LIGA (Lithographie, Galvanoformung, Abformung)

LIGA is a German acronym for lithography, electroplating, and molding. It is a process that is capable of making small complex structures of electroplateable metals with very high aspect ratios (structures that are much taller than wide) with thicknesses up to millimeters [3].

It uses x-ray lithography, thick resist layers, and electroplated metals to form complex structures. The process starts with a sheet of Polymethyl Methacrylate (PMMA). This sheet is covered with a photomask and then exposed through radiation. The exposed PMMA is then etched away and it leaves vertical walls in the structure that are very accurate. Metal is then plated into the structure to replace the PMMA that was etched away. The metal is the final part of the LIGA process. From this, they can fabricate an injection mold made of metal which then can be used to form parts typically made with plastic. LIGA was first developed in the 1980's and further developed in the 1990's and early 2000's by Sandia National Laboratories. The LIGA process is appropriate when you need higher aspect ratios than those obtainable from surface micromachining. Table 2.1 summarizes the three fabrication technologies for MEMS devices and the specialized equipment needed to process the devices.

Fabrication Technology	Process Equipment
Sacrificial Surface Micromachining	Release and drying systems to realize free-standing microstructures
Bulk Micromachining	Dry etching systems to produce deep, 2D free-form geometries with vertical sidewalls in substrates Anisotropic wet etching systems with protection for wafer front sides during etching Bonding and aligning systems to join wafers and perform photolithography on the stacked substrates
LIGA Micromolding	Batch-plating systems to create metal molds in LIGA process Plastic injection molding systems to create components from metal molds

Table 2.1 Summary of Process Equipment Specific to MEMS [13].

2.5   Sandia National Laboratories MEMS Fabrication

Sandia National Laboratories has been investing in the development of small CMOS compatible MEMS resonators and filters. The common MEMS processes, as described previously, can not achieve low impedance filters and are not post-CMOS compatible. Therefore, a post-CMOS compatible aluminum nitride (AlN) MEMS resonator process

was developed [14]. This process is defined as a simple four-mask, low-temperature, and CMOS compatible (Tmax < 350 °C) process. This process flow has been used to fabricate MEMS devices and uses conventional surface micromachining techniques to manufacture high quality AlN resonators with high yield [15]. The process flow is shown in Figure 2.1.

The process replaces the platinum bottom electrode with standard CMOS metals, aluminum (Al) and tungsten (W). (a) The process begins with an anisotropic silicon (Si) etch and the deposition of a thin oxide to isolate the bottom electrode from the substrate. Tungsten is then deposited and polished until it remains only where Si was etched above. An oxide touch polish is then performed to further smooth the top of the wafer prior to AlN deposition. A 50 nm Al bottom electrode is deposited and patterned prior to sputtering 750 nm of AlN at 350 °C. AlN is piezoelectric and is used to drive and sense the resonators. Using this process, highly oriented c-axis AlN films with a rocking curve full width half maximum of < 1.5° measured using x-ray diffraction can be reliably formed. (b) Contacts to the W areas are etched in the AlN and a 100 nm thick Al top electrode is deposited and patterned. (c) Finally, the resonator frequency is defined by etching trenches in the AlN down to bulk Si and the devices are released in dry SF_6. The maximum temperature in this process is 350 °C and all of the materials, SiO_2, Al, W, and AlN are CMOS compatible and can be deposited and etched using standard CMOS tools.

It is important to note that the processing of the devices is dependent on the width/length and not height dependent.
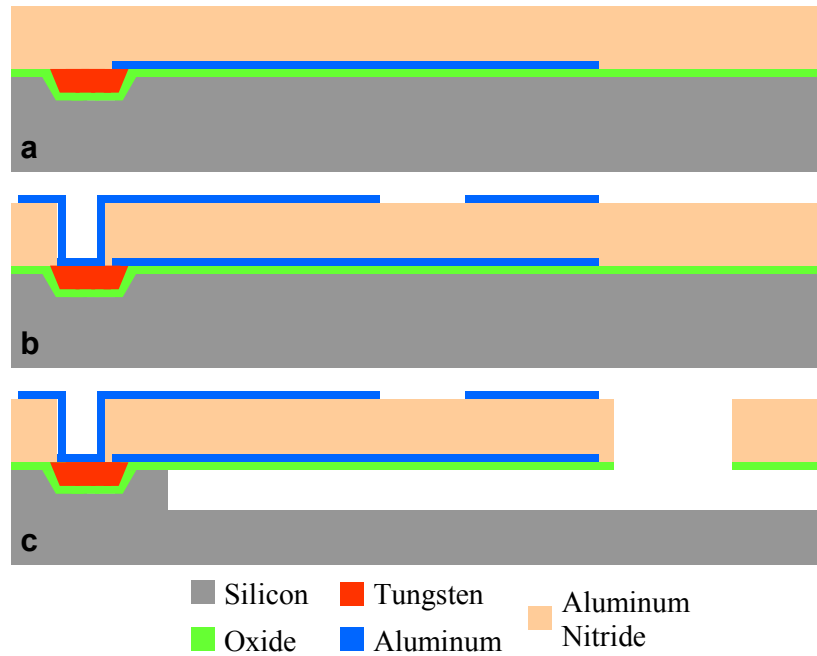
Figure 2.1 Aluminum Nitride Microresonator Process Flow.

2.6   Dual Mode Aluminum Nitride Filter

The process that is shown in Figure 2.1 is the process that was used to develop the dual mode Aluminum Nitride (AlN) Filter that was shown previously in Figure 1.4. It is shown in Figure 2.2 for convenience. This dual mode filter is a new technology in the RF MEMS filter area.
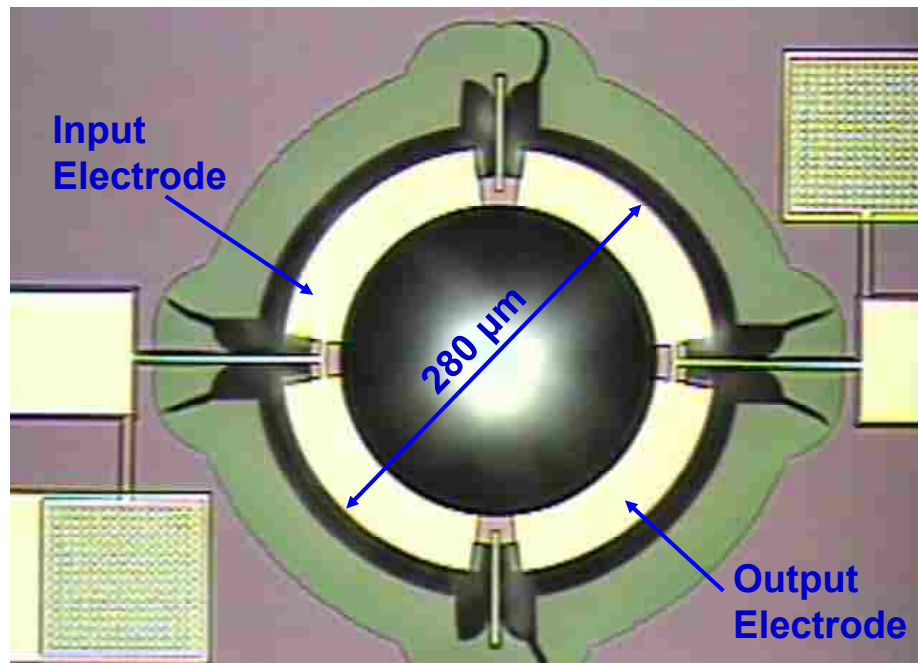
Figure 2.2 Dual Mode Aluminum Nitride Band Pass Filter.

The device utilizes two closely spaced modes to achieve a band pass response in a single device. These devices are built to specifications based on width/length as compared to height. These devices have features just big enough for good performance, yet small enough to achieve higher frequencies. These features will be discussed later in this thesis. Figure 2.3 shows the two mode shapes of the dual mode filter. The MEMS filter that is shown here is integrated into a 5-channel filter on one chip that is the baseline for this thesis.

f_{mode1}= 108.18 MHz f_{mode2}= 108.66 MHz
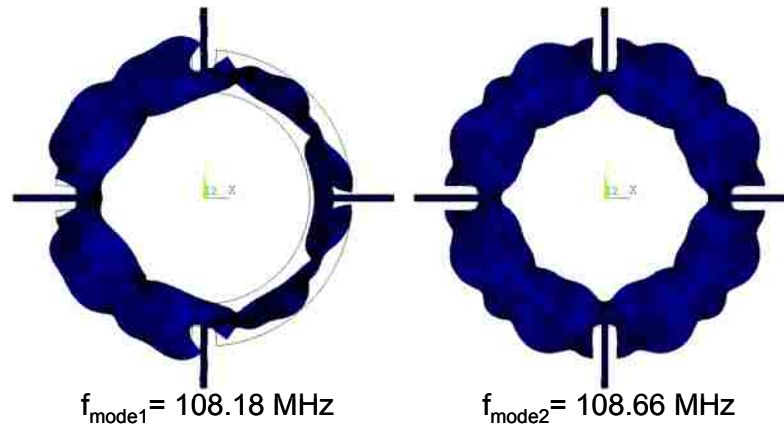
Figure 2.3 Simulation showing the two mode shapes of the AlN dual mode filter.

2.7   Summary

This chapter presented the various technologies used to develop IC's and MEMS. As previously discussed, MEMS fabrication uses many of the materials and processes of semiconductor fabrication, but there are important distinctions between the two technologies. The basic challenge of using semiconductor processes for MEMS fabrication is not so much in the type of processes and materials used, but more in the way those processes and materials are used.   Once the basic MEMS processes were established, Sandia National Laboratories was able to expand on that technology to produce MEMS resonators and filters. The filters are still in a research stage, but are the basis for this thesis. In the following chapters, we will further explore the characteristics that these filters have and implement them into a full communication system.

Chapter 3

MEMS Devices

The primary focus of this chapter is to understand the MEMS devices, mainly the MEMS filter, that have been created at Sandia National Laboratories. These devices are constantly being experimented with to meet design parameters so our discussion will be limited to the first set of filters that were designed. This chapter will also discuss how the filters are to be simulated in MATLAB. The results of the simulations will be compared to actual results of the filters that were designed. This simulation is of interest because it provides the baseline for this thesis. Without a working simulation of the filters, it is not possible to develop a full BPSK communications system. Additionally, the work developed in Chapter 3 will be further analyzed in Chapter 4 of this thesis, which contains BPSK simulation results of the filters in a full communications system. Chapter 4 will also show a comparison of the actual devices implemented on a test board.

This chapter is organized as follows. First the MEMS filters will be described with regards to development and performance. Then the MEMS filters will be shown as the equivalent circuit in a circuit theory discussion. The nodal equations will be developed and this will help aid in the process to simulate the MEMS filters in MATLAB. The results will be shown in comparison to actual results from a 5-channel

MEMS filter bank. The final result is necessary to implement the device into a BPSK communication system.

3.1   The MEMS Filter

A MEMS development area that is receiving a lot of attention in industry is the RF MEMS area. The goal is to be able to create a single-chip that includes resonators, filters, switches and other IC electronics. If RF MEMS can be produced on a single chip, the advantages for daily items such as the cell phone would be better performance at a lower cost. It has been and still is a technical challenge to develop these items. Sandia National Laboratories has taken a step by developing a post-CMOS compatible filter. These filters entail a form of wave propagation at some stage between their input and output terminals. These waves are usually vibrations amongst the different modes. Most RF communication systems have a need for band pass filters with an extremely narrow pass band and rapid roll off on either side of the pass band [4]. This is accomplished by these filters.

The important characteristic of a filter is the insertion loss. This is the ratio of the signal at the output with respect to the filter at the input. Insertion loss in filters is usually defined in decibels (dB). This can be found by the following equation:

$$\text{Insertion loss (dB)} = 20 \log (V1/V2) \tag{3.1}$$

where V1 is the signal level in a test configuration without the filter installed, and V2 is the signal level with the filter installed.

The pass band characteristics of a filter are generally expressed as a quality factor (Q-factor). The Q-factor is a measure of the energy stored in the system to the energy dissipated. It is defined as:

$$Q = \frac{fo}{\Delta f} \tag{3.2}$$

where *fo* is the center frequency and $\Delta f = f_2 - f_1$. The equation shown gives the user an idea of the filter's effectiveness in the frequency response.

Other important characteristics that define filters are stop band rejection, roll off rate, bandwidth, and in our case, the filter size. The stop band rejection is the signal transmitted through the system at frequencies beyond the pass band. This also is expressed in dB. The roll off rate is the rate at which the transfer response of the filter changes from pass band to stop band. Bandwidth is the frequency range at which our filter operates.

The filter size is one of the key aspects in pursuing microresonator based filters. If MEMS based filters are able to be produced as post-CMOS compatible, the industry would be able to replace current technologies such as surface acoustic wave (SAW) and

quartz filters with MEMS filters. The size of MEMS filters leads to smaller parts and this in turn leads to radio miniaturization, but also enables large banks of filters to be integrated on the same substrate. This would allow multi-channel radios or real time spectral analysis on a single chip [16]. Another advantage of fabricating these chips through the aforementioned technology is the ability to produce hundreds of these tiny filters on one single chip. This would replace off-chip filters, resonators, and mixers reducing the physical size needed by RF hardware.

As discussed in Chapter 2, Sandia National Laboratories has invested in the development of a dual mode MEMS filter. These filters are piezoelectric devices. Piezoelectricity refers to the ability of certain types of materials to change shape with the application of electrical voltage or, conversely, to produce an electric charge as a result of these mechanical changes. Sandia National Laboratories has taken advantage of this piezoelectric effect to develop these filters. These filters implement a 4th order bandpass filter using a single resonator for reduced size [16]. Figure 3.1 shows the dual mode MEMS filter with filter dimensions. The mechanical properties of these filters depend on the shape and modes of vibration. By simply tweaking the radius (R) or width (W), we can change the frequency and other properties of the filters. A common parameter to adjust the frequency is the width. The first set of filters that were created were based on selecting an arbitrary width. As shown in the picture, 41 microns is the width. This was a nice round number that created a frequency in the 110 MHz range. We will discuss this

in more detail later. Also, if you place the electrodes in different locations, you can sense

different phases of the electric wave generated. Simple techniques such as these change

the mechanical properties of the MEMS filters. This will be discussed in more detail

later in this Chapter. Figure 2.3 showed the two modes of vibration that can be achieved

with the AlN MEMS filter. This is shown in Figure 3.2 for convenience.
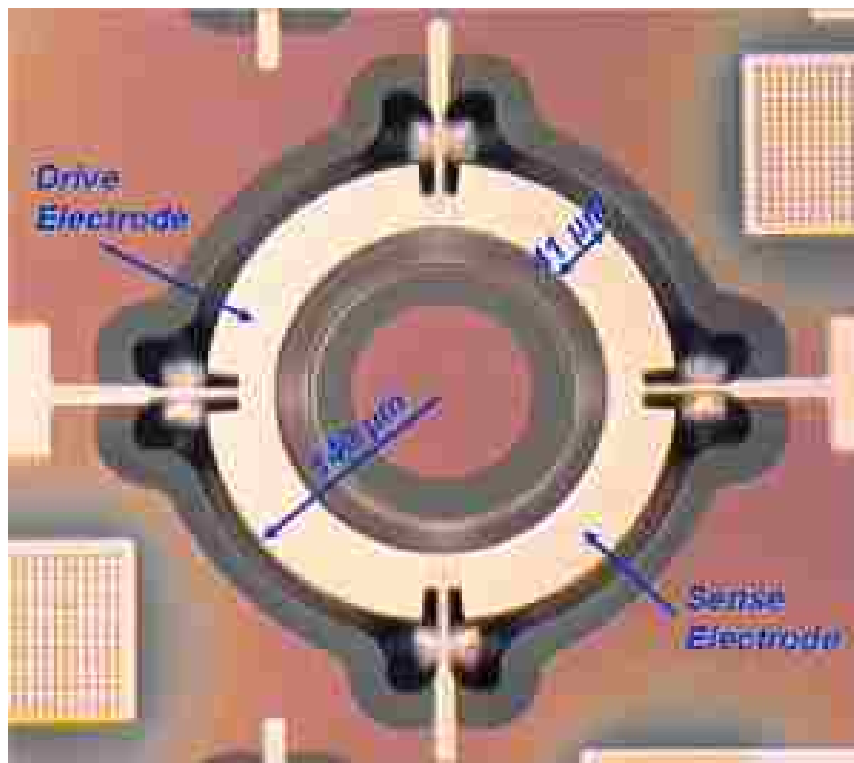

Figure 3.1 Picture of AlN dual mode MEMS filter. R is 140 μm and W is 41 μm
(Courtesy of Sandia National Laboratories).

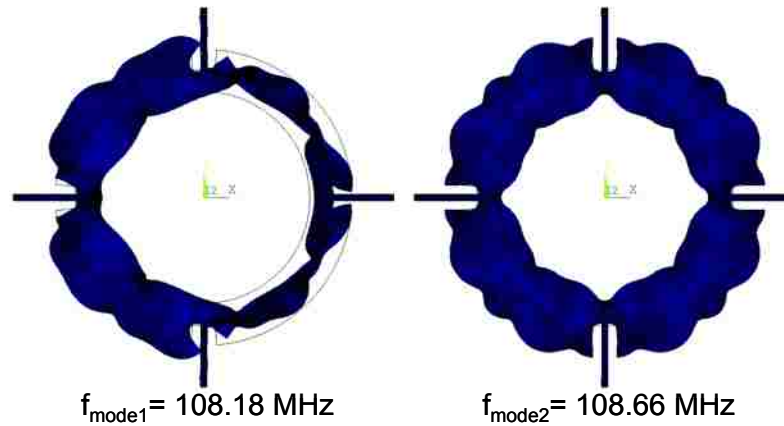f_{mode1}= 108.18 MHz f_{mode2}= 108.66 MHz

Figure 3.2 Simulation showing the two mode shapes of the AlN dual mode filter.

The dual mode filter operates by closely spacing the frequencies of two resonant modes in a single device. While dual mode filters have been previously reported at lower frequencies [17], this filter utilizes the mode shapes shown in Fig. 3.2, which is appropriate for realizing low impedance filters at frequencies in excess of 100 MHz [16].

The loaded Q's of the two modes for the MEMS filters have been recorded at 800 and 1000. The two modes that are shown in Fig. 3.2 represent the mode shapes where the sense half of the ring vibrates out of phase with the drive while the other mode is the mode shape where the drive and sense halves of the ring vibrate in phase. The bottom electrode is grounded in this configuration which significantly reduces the feedthrough capacitance between the drive and sense electrodes, vastly increasing the filter stop band rejection.

28

The dual mode filter is a reciprocal device allowing the drive and sense electrodes to be interchanged. The filter passband is located at approximately:

$$f \approx \frac{1}{2W} \sqrt{\frac{E}{\rho}} \qquad\qquad (3.3)$$

where W is the width of the ring shown in Figure. 3.1 and E and ρ are the effective Young's modulus (225 GPa) and density (2956 kg/m3) of the resonator film stack.

Increasing the radius of the filter decreases the resonant frequency for both modes but at a different rate, allowing the filter bandwidth and center frequency to be independently set by adjusting W and R [16]. The smaller the width, the higher the frequency, but the trade off is more insertion loss. The devices explored in this work have filter frequencies between 105 – 115 MHz. This will be discussed later. The design is completed by anchoring the dual mode filter using notched supports in the middle of the ring which is a nodal point of zero displacement using beams sized to be an odd multiple of a quarter wavelength for both compression and flexural modes. Using this anchoring scheme minimizes acoustic losses to the substrate [16]. As you can see, a lot of work has gone into developing this device with very good results so far. The next step is to apply these devices and see how they react with real world systems.

3.2   Performance Analysis

In this section, the results of a single dual mode MEMS filter are presented. The section will display how a single MEMS filter can be integrated into circuitry and be measured. The simulated response and measured response will be shown of a single MEMS filter. Finally, some measured filter specifications will be displayed.

Figure 3.3 shows the dual mode filter in a circuit with termination. You can see that this termination is not the normal 50 Ω termination. Matching integrated circuits to 50 Ω off-chip components requires power hungry circuitry. Because MEMS filters are so small and they can be placed so close to the integrated circuits, the power saved is an advantage. This is desirable because you want to operate on an impedance standard higher than 50 Ω, because 50 Ω drivers consume large amounts of power and matched lines are not necessary in integrated transceivers where the line length between components is less than 1 mm [14]. As mentioned previously, MEMS devices can replace the need of off-chip components. This single MEMS filter is conveniently set up so that you are able to measure the input and output of the MEMS filter, easily change out the termination resistors, and do any type of testing necessary to validate the characteristics of the single MEMS filter. This was done for simple evaluation purposes.
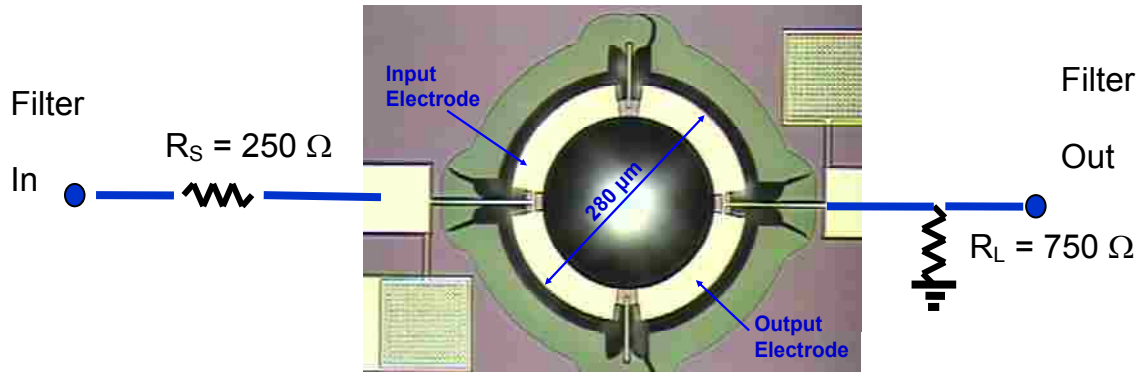
Figure 3.3 Photo of dual mode AlN nitride filter.

The measured response of the dual mode filter is shown in Figure 3.4. This compares the measured filter with the modeled filter. The measured response is with a 50 Ω termination resistor. The simulated response is based on a 4th order differential equation from two equivalent RLC networks. This will be discussed in further detail in the next section. Table 3.1 is a summary of important characteristics that were measured from the dual mode filter. This table was measured with the circuitry of Figure 3.3. As mentioned previously, this termination scheme is optimal because it is operating on an impedance higher than 50 Ω. The table includes some of the important characteristics of filters as previously discussed. As you can see from the results, the filter is able to achieve the desired results as expected.
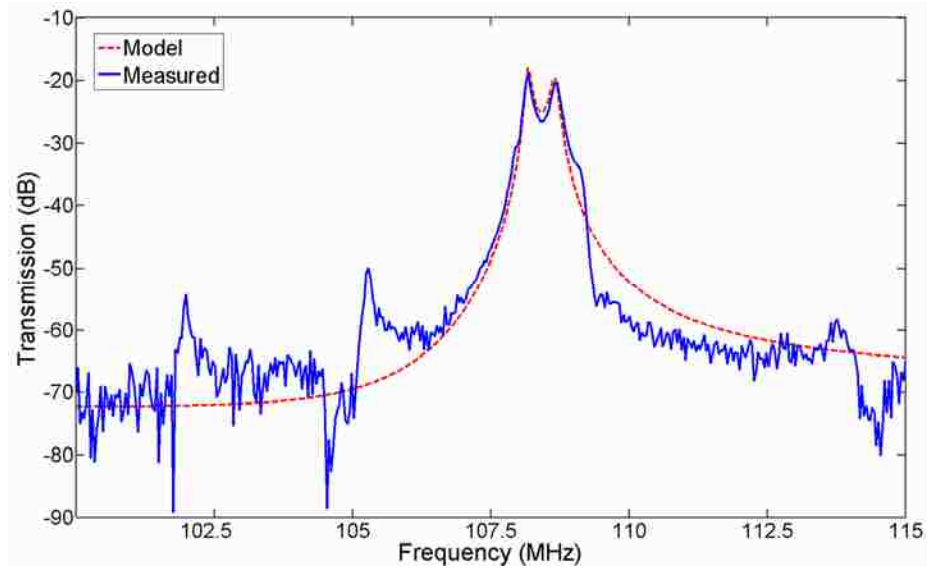
31

Figure 3.4 Measured and simulated response of dual mode filter.

Insertion Loss	5.7 dB
Center Frequency	108.5 MHz
Bandwidth	675 kHz
Ripple	1.37 dB
Stop Band Rejection	$\approx$ 40 dB
20dB Shape Factor	2.7
Termination Resistors	250 Ω 750 Ω
Filter Size	0.062 mm^2

Table 3.1 Dual mode measured filter specifications.

3.3   Equivalent Circuit

Mechanical properties of resonators depend on their shape, type of material used and the relevant modes of vibration. Modeling of these systems is generally done by using their equivalent circuits, which can be translated to the electrical domain by simple transformations for design and optimization.   Figure 3.5 shows the equivalent circuit model of the dual mode AlN MEMS filter.   The circuit elements within the square represent the components inherent to the filter. The transformer captures the 180° phase between modes. Table 3.2 shows the values of all components for filter center frequency of 108.4 MHz.
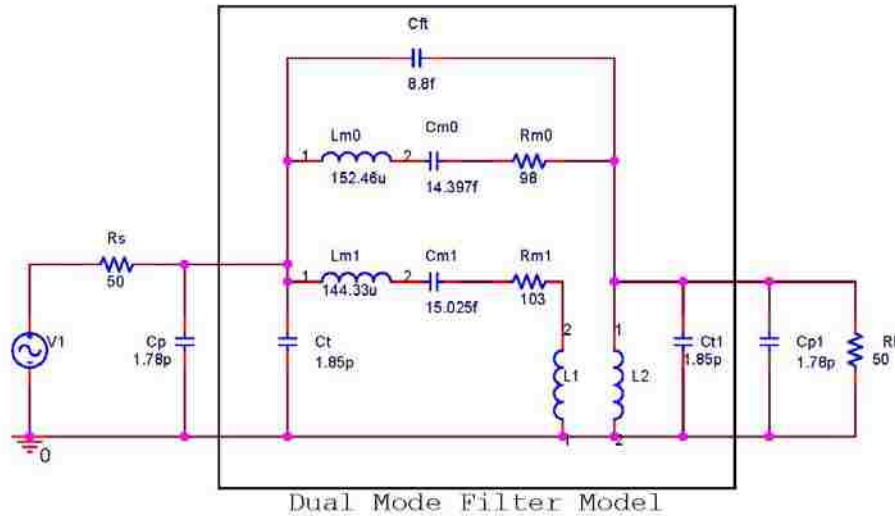

Figure 3.5 Equivalent Circuit Model of Dual Mode Filter.

Circuit Element	Value
L_{M0}	151.41 µH
C_{M0}	14.302 fF
R_{M0}	98 Ω
L_{M1}	143.65 µH
C_{M1}	14.949 fF
R_{M1}	103 Ω
C_{FT}	8.8 fF
C_T	1.85 pF
C_P	1.78 pF
R_S	50 Ω
R_L	50 Ω

Table 3.2 Circuit Component Values.

This filter represents a radius of 140 μm and a width of 41 μm. This frequency can be changed by changing various components to equivalently change the size and shape of the resonator. As mentioned previously, this is done by adjusting the radius or width of the actual filter. So to tweak the frequency, we play with the MODES of the device. Since these are piezoelectric devices, they are comparable to waveguides. As with waveguides, the piezoelectric mode frequencies (fundamental and other harmonics) are determined mostly by the size and shape of the piezoelectric material (and the material properties). Also, similar to wave guides the electrodes can be placed in different locations to sense different phases of the electric wave generated. Although, when you

try to get different phases, you'll also receive different amounts of power. This is unlike a waveguide, because as you move a feed down a waveguide (so long as the feed is at the mode profile maximum) you can always receive the same amount of power. As these parts physically vibrate, the piezoelectric effect creates an output current. These devices are purely designed with mechanical resonances. The theory seems simple, but there are many factors to worry about to get these devices to operate consistently and efficiently.

In order to change the frequency in the equivalent circuitry, you need to solve for the new values of L and C. This will adjust the size of the resonator. The components that correspond to adjusting the size of the resonator in the equivalent circuit are L_{M0}, L_{M1}, C_{M0}, and C_{M1}. There are two assumptions that are made here before proceeding. These two assumptions are:

- The Q factor remains constant
- The Insertion Loss remains constant

Therefore to change the resonant frequency, we use the following equations:

$$L_{new} = L_{old} \frac{F_{old}}{F_{new}} \tag{3.4}$$

$$C_{new} = \frac{1}{L_{new}(2\pi F_{new})^2} \tag{3.5}$$

Chapter 3. MEMS Devices

The frequencies of interest for this simulation are based on the actual MEMS filter that has already been created. As mentioned previously, these frequencies were chosen based on a convenient W value to start (i.e. 40, 41, or 42 microns would be used because they are nice round numbers) that would produce a frequency in the 110 MHz range. As the experimentation became more advanced, the width was adjusted to meet the desired frequencies. The frequencies of interest for the simulation are 107.75, 109, 110.25, 111.50, and 112.75 MHz. The desired bandwidth is ~650 kHz. The new values calculated are shown in Table 3.3.

Desired Center Frequency (MHz)	107.75	109.00	110.25	111.50	112.75
L_{M0}	152.46 μH	150.71 μH	148.99 μH	147.32 μH	145.68 μH
C_{M0}	14.397 fF	14.231 fF	14.070 fF	13.911 fF	13.757 fF
L_{M1}	144.33 μH	142.68 μH	141.07 μH	139.49 μH	137.95 μH
C_{M1}	15.025 fF	14.853 fF	14.685 fF	14.521 fF	14.361 fF

Table 3.3 New Inductor and Capacitor Values.

3.4   Simulation Results

The calculated components were inserted into a software program called PSPICE to simulate the expected output of the circuit. This is to verify that the frequency of the filter is as expected. The convenience of using a SPICE program is it develops a netlist which can be readily converted into the MATLAB program as will be seen later.
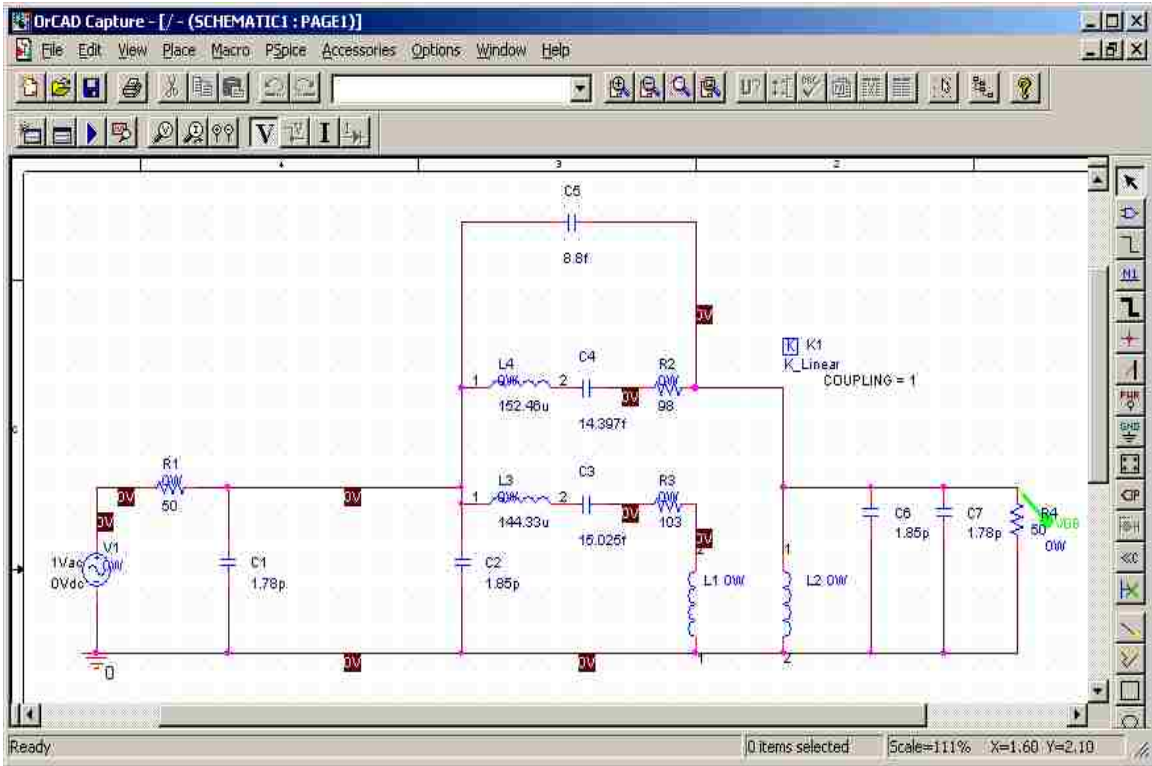

Figure 3.6 Equivalent Circuit Model of Dual Mode Filter.

37

The next step is to simulate the circuit in MATLAB so it can be implemented in a system. There are several ways to try to accomplish this. The first way is to take the equivalent 2 RLC networks that represent the dual mode filter, which is governed by a 4th order equation, and derive this in MATLAB. The second way is to do nodal analysis on the equivalent circuitry. Since there are 5 filters that need to be modeled, the latter way was chosen to make the process more automated. Eight nodes have been chosen to evaluate. The method to evaluate the circuitry will be done by a process of Modified Nodal Analysis (MNA) [18]. The general steps that are involved in MNA are provided here:

1. Select a reference node (usually ground) and name the remaining n-1 nodes.
2. Assign a name to the current through each voltage source.
3. Apply Kirchoff's current law to each node.
4. Write an equation for the voltage for each voltage source.
5. Solve the system of *n-1* unknowns.

By following this process by hand, you will see that you can develop several matrix equations. From these equations, there are several patterns that become apparent. These patterns are crucial in developing an algorithm for MNA. The first apparent pattern is: All of the circuits resulted in an equation of the form [18].

$$A x = z \tag{3.6}$$

From this equation, we know that we can use a powerful tool such as MATLAB to manipulate matrices that equate to Equation 3.6. Figure 3.7 is a simple example of a Modified Nodal Analysis (MNA) circuit and Figure 3.8 shows the corresponding matrix. The simple circuitry and simplistic nodes will give you an idea of how to apply this analysis and develop the netlist for the program. By examining Figure 3.8, you can start to see the pattern developing. This will be explained in further detail below.
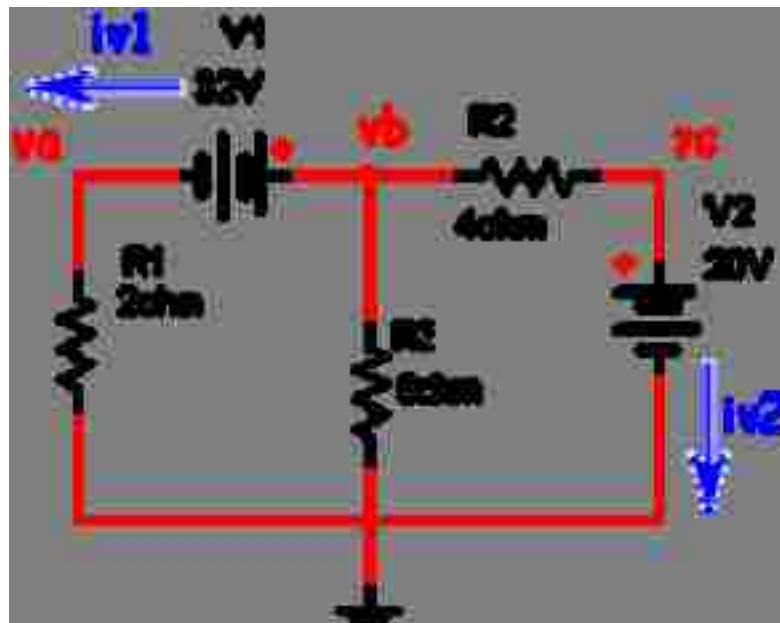

Figure 3.7 Simple Circuit to Demonstrate MNA [18].

$$\begin{bmatrix} \dfrac{1}{R_1} & 0 & 0 & -1 & 0 \\ 0 & \dfrac{1}{R_0}+\dfrac{1}{R_9} & -\dfrac{1}{R_9} & 1 & 0 \\ 0 & -\dfrac{1}{R_9} & \dfrac{1}{R_9} & 0 & 1 \\ -1 & 1 & 0 & 0 & 0 \\ 0 & 0 & 1 & 0 & 0 \end{bmatrix} \begin{bmatrix} v\_1 \\ v\_2 \\ v\_3 \\ i\_v1 \\ i\_v2 \end{bmatrix} = \begin{bmatrix} 0 \\ 0 \\ 0 \\ v1 \\ v2 \end{bmatrix}$$

Figure 3.8 Matrix results of MNA Analysis on Circuit Shown in Figure 3.7 [18].

The A matrix is defined by [18]:

1) $(n+m)*(n+m)$ in size, and consists only of identified quantities

2) the nxn part of the matrix that is in the upper left:

   a) has only passive elements

   b) has elements connected to ground appear only on the diagonal

   c) has elements that are not connected to ground as both diagonal and off-diagonal terms

3) the rest of the **A** matrix (not included in the nxn upper left part) contains only 1, -1, and 0

The **x** matrix is defined by [18]:

1) an $(n+m) * (1)$ vector that holds the unknown quantities (node voltages and the currents through the independent voltage sources).

2) the top n elements are the n node voltages.

3) the bottom m elements represent the currents through the m independent voltage sources in the circuit.

The **z** matrix is defined by [18]:

1) an $(n+m) * (1)$ vector that holds only known quantities

2) the top n elements are either zero or the sum and difference of independent current sources in the circuit.

3) the bottom m elements represent the m independent voltage sources in the circuit.

Finally, the circuit is solved by a simple matrix manipulation:

$$x = A^{-1}z \tag{3.7}$$

The solved result shows the voltages and currents of the respective nodes. There is currently a MNA tool that is readily available to process these types of circuits. This program is called Symbolic Circuit Analysis in MATLAB (SCAM). This program takes a circuit analysis netlist that the user defines and symbolically solves for the voltages and currents of the respective nodes. Once these values are known in MATLAB, we can use
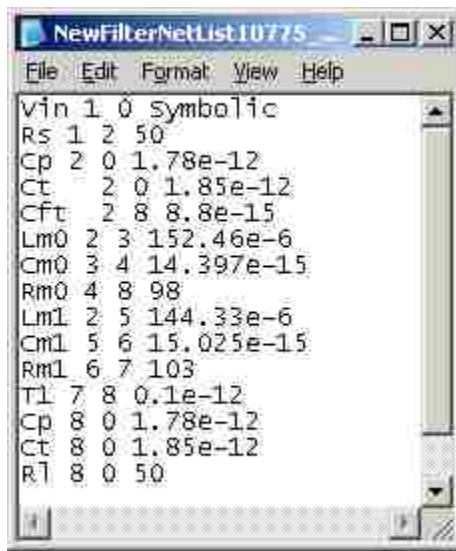
the values and manipulate them for other things. In our case, we want to find the transfer

function of the filter. From this transfer function, we are able to plot the result and see if

the filter is equivalent to the circuitry that we designed. The original SCAM MATLAB

code is a generic set of code that is compatible with certain components, such as

Resistors, Inductors, Capacitors, and Op-Amps. This code did not include a transformer

function that we have in our circuitry. In order to make this code work, we needed to

modify the code. The code that was added to help with the transformation of the

transformer is shown below:

```matlab
    case 'T'
        g = ['1/s/' Element(i).Name];
end

%If neither side of the element is connected to ground
%then subtract it from the appropriate location in the matrix.
if (Element(i).Name(1)=='T')
   G{n1,n2} = [G{n1,n2} '+'  g];
   G{n2,n1} = [G{n2,n1} '+'  g];
elseif (n1~=0) & (n2~=0),
   G{n1,n2}=[ G{n1,n2} '-' g];
   G{n2,n1}=[ G{n2,n1} '-' g];
end

%If node 1 is connected to ground, add an element to the diagonal
%of the matrix.
if ((n1~=0) || (Element(i).Name(1)=='T'))
   G{n1,n1}=[ G{n1,n1} '+' g];
end
%Same for node 2.
if ((n2 ~= 0) || (Element(i).Name(1)=='T'))
   G{n2,n2}=[ G{n2,n2} '+' g];
end
```

Now that we have the code needed to simulate the 5-channel MEMS filter, we need to develop the netlist for each filter. This is accomplished by running 5 separate PSPICE models with the correct values obtained from Table 3.3. An example of the netlist created is shown in Figure 3.9.

Figure 3.9 Netlist Result of 107.75 MHz MEMS Filter.

This has laid the groundwork for the simulation of the 5-channel MEMS filter. The netlist file is created in .txt format and is defined by the user with the appropriate component values. SCAM accepts the .txt file and uses the appropriate data to run it through the code. The SCAM program returns the transfer functions and evaluates them symbolically.   Once the results are shown symbolically, I take those results and

manipulate them into a form that is MATLAB friendly. These results are plotted for

visual comparison. This process is re-run 5 times to generate the 5-channel MEMS filter

bank. The MEMS filter bank that will be simulated has frequencies of 105.5, 106.75,

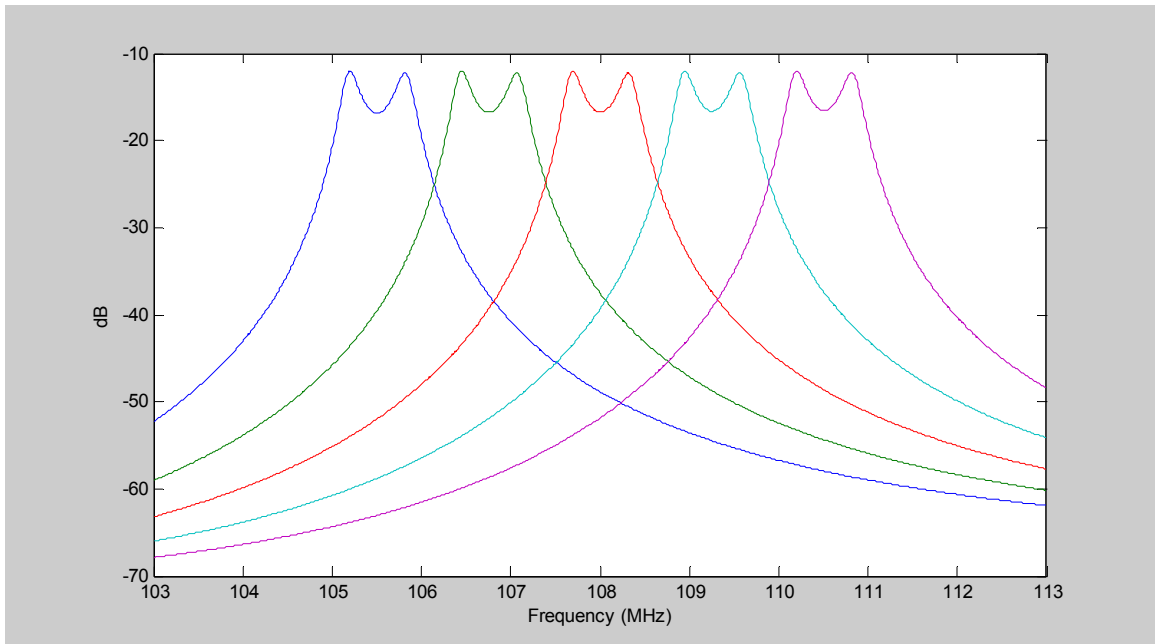108, 109.25, and 110.5 MHz. The results are shown in Figure 3.10.

Figure 3.10 Simulated Results of 5-Channel MEMS Filter Bank.

Now that we have simulated the 5-channel filter bank, we need to verify that our

results are representative of a real filter bank. The next figure, Figure 3.11, shows the

measured results of 5-channel MEMS filter bank. As you can see from the Figures, the

simulated results are validated by the actual measurements. The actual filter banks seem

to have a narrower bandwidth for each channel when compared to the simulated results. This is caused by a parasitic resonance amongst the dual modes. You'll also notice there is ~5 dB difference in filter insertion loss between the two figures. This characteristic is not as important as the shape of the experimental curves. But, the overall filter shape is consistent for each simulated and measured channel.
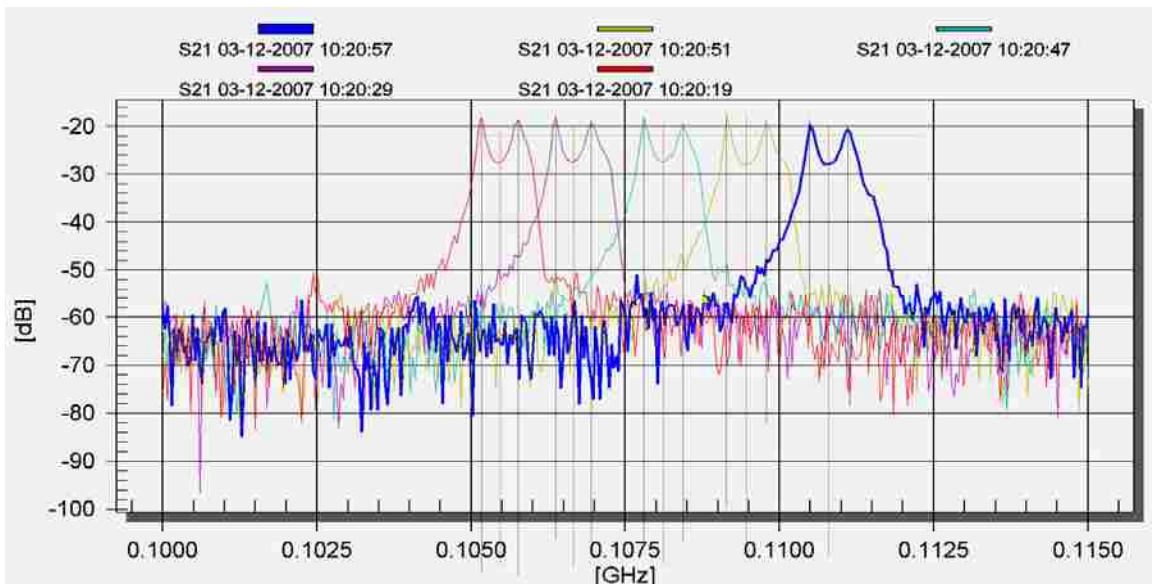

Figure 3.11 Measured Results of 5-Channel MEMS Filter Bank.

3.5   Summary

This chapter illustrated the particular design of a MEMS filter that was fabricated at Sandia National Laboratories. It showed the equivalent circuitry that was used to develop and simulate a dual mode MEMS filter with frequency ranges in the 100 MHz.

Furthermore, it provided an analysis of the simulated 5-channel filter bank with comparisons to an actual 5-channel filter bank that was measured.

This chapter has provided further insight into the performance of the MEMS filters. The designer can now feel confident that what is being simulated accurately represents the actual device. However, this performance analysis might not be enough since it does not insert actual RF channel effects such as noise, interference, or phase noise.

The following chapter extends the performance analysis to a BPSK system. This system will introduce random noise and be tested as a whole system. Once this is simulated through MATLAB, a comparison will be made to an actual bench setup. This will validate what is being simulated to the real world scenario. The RF channel effects of phase noise, interference, etc. will be of interest. Furthermore, this simulation provides a good baseline for what can be accomplished in future systems. In particular, the models will give the user a good idea of how certain RF channel effects will affect the system.

Chapter 4

BPSK Analysis

This chapter extends the performance analysis of Chapter 3 by presenting a performance analysis based on MATLAB simulation results. The MATLAB simulations will consist of modeling a BPSK receiver and transmitter, with the MEMS filter included in that simulation. First, the simulations that were created in Chapter 3 must be manipulated to be usable in the time domain. These filters will also be mixed down to baseband like they would in a real system. Once this is accomplished, a MATLAB simulation of the transmitter must be created. It will be shown that the simulation of the transmitter will include random noise and we'll have signals that represent real scenarios. Next, a receiver with the MEMS filters implemented will be developed and simulated. The results of the transmitter and receiver will be presented as a whole BPSK system.

These results of the simulated wireless system should be able to be replicated with an actual system. Therefore, a real system will be implemented using an actual MEMS device and test board. The receiver from the simulation will be implemented in MATLAB. The results will be presented and you can make a comparison from the simulation.

4.1 Simulations

The overall simulation is going to be set up in a main simulation function and then it calls on the transmitter and receiver functions. In the main simulation function, the MEMS filter array is set up from the previous simulation in Chapter 3. The function has some initial setup where frequencies are normalized and initialization parameters are defined. The simulation function also has the job of sending the information back and forth between the functions. The final thing the simulation function does is plot the final constellation diagram.

The first step to setting up the simulation is manipulating the MEMS 5-channel filter bank and passing the correct data from the MEMS filters. As was seen in Figure 3.10, the MEMS device is operating in the $103 - 113$ MHz range. For this portion of the simulation, the frequencies have been adjusted to match the set of filters that were available to test on the actual test board. These frequencies are in the $105 - 115$ MHz range. This filter bank is shown in Figure 4.1. This filter bank needs to be manipulated before it can be loaded into the simulation function. Some of the manipulations that need to occur are getting it in the right domain and normalizing the frequency. Those manipulations will follow in the next few sections, along with the development of the transmitter and receiver function.
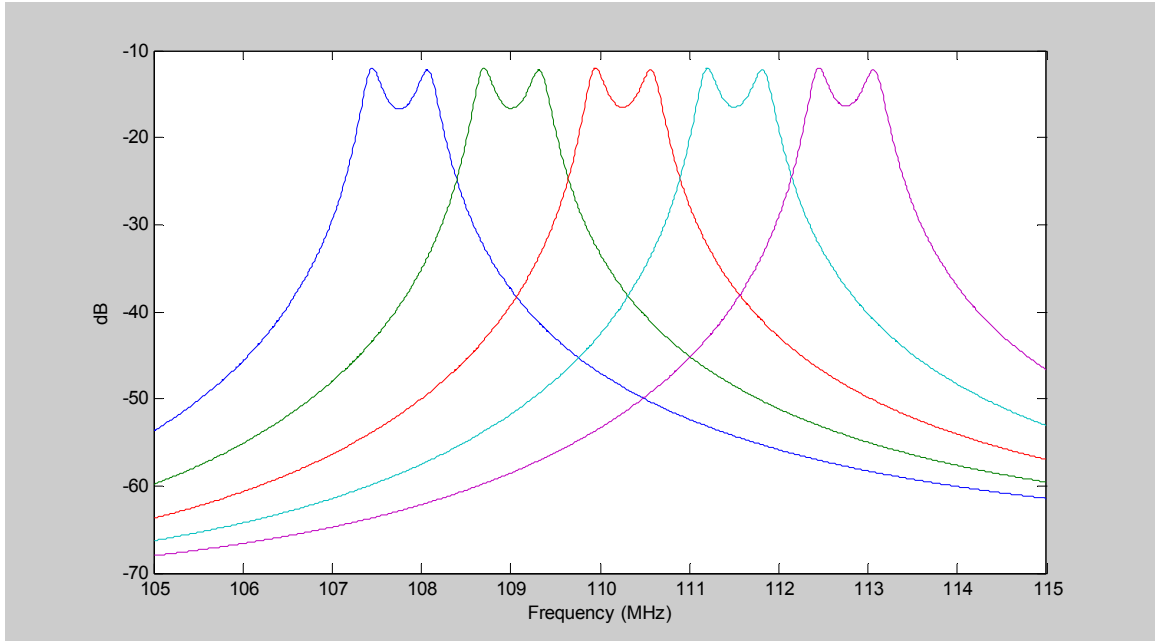
Figure 4.1 Test Board Simulated MEMS 5-Channel Filter.

As mentioned previously, the filter banks need to be manipulated to be compatible with the receiver and transmitter. The first issue is the domain that the filter bank is in. It is currently observed that these signals are in the s-domain. In order to digitally use these signals in a system, we need to transfer them to the z-domain. This can be accomplished by using the Bilinear z-transformation or the Inverse Discrete Fourier Transform (IDFT). The first method described is the Bilinear Transform. The equation below transforms analog filters that were designed by classical filter techniques into their discrete equivalents. It maps the s-plane into the z-plane by:

$$H_d(z) = H_c(s)\Big|_{s = \frac{2}{T}\frac{1-z^{-1}}{1+z^{-1}}} \tag{4.1}$$

where T is the sample time. It also creates a relation between the analog frequency variable, Ω, and the digital frequency, $\acute\omega$, by mapping the $j\Omega$ axis (from $\Omega = -\infty$ to $+\infty$) repeatedly around the unit circle ($e^{j\acute\omega}$, from $\acute\omega = -\pi$ to π) by [19]:

$$\omega = 2\tan^{-1}\left(\frac{\Omega T}{2}\right) \tag{4.2}$$

The Bilinear transform method was attempted on the simulated filter bank transfer functions. The numerical values of each channel in the filter bank transfer function are very big numbers. Some of the coefficient weights in the numerator range from 10^{148} to powers of 10^{151}. The same holds true for the coefficient weights of the denominator. These values range in powers of 10^{161}. Due to this large number, when the bilinear transformation is applied, we lose the significance of the numbers and we get large numerical inaccuracies.

The Fourier transform method takes a signal in the time domain and maps it into the frequency domain. The frequency domain representation is the exact same signal, but in a different form. The inverse Fourier transform maps the signal back from the frequency domain into the time domain. The Fourier transform maps the time domain sequence into a frequency domain sequence, where each value is a complex number that is associated with a given frequency. The inverse Fourier transform takes the frequency

sequence of complex values and maps them back into the original time sequence. The result of the IDFT will be complex numbers where the imaginary part is zero. By doing this method, we can find all the parts of the filter where it is "Not A Number (NAN)" in MATLAB and use this information accordingly. Either of these two methods is valid, but since the bilinear transformation created large numerical inaccuracies, the IDFT method was used for this thesis. The tradeoff is in the IDFT method we have to sample it a lot, but this is much better than the numerical inaccuracies.

Once the filter bank is transformed into the correct domain, we have to normalize the frequency. In the analog realm, a signal frequency is measured in hertz (Hz). In the digital realm, a system uses a digital frequency. This is the ratio between the analog frequency and the sampling frequency. It can be shown by the following equation:

$$f_d = \frac{f_a}{f_s} \tag{4.3}$$

where f_d is the digital frequency, f_a is the analog frequency, and f_s is the sampling frequency. The digital frequency is known as the normalized frequency and is measured in cycles per sample. The normalized frequency ranges from 0.0 to 1.0, which corresponds to a real frequency range of 0 to the sampling frequency f_s. The normalized frequency also wraps around 1.0 so a normalized frequency of 1.1 is equivalent to 0.1.

We need to manipulate the MEMS filter bank to mix down the frequency from the 100 MHz range into baseband. By doing this, we are also able to get a reasonable amount of samples when we are simulating it. After the frequencies have been mixed

51

down and normalized, we can plot the data to view the simulated filters in MATLAB.

The predefined function that is set up in MATLAB is the "fvtool" function. The "fvtool"

is used by MATLAB to help the user analyze digital filters. Figure 4.2 shows the first

filter in the 5-channel filter bank that has been normalized. Each of the filters was

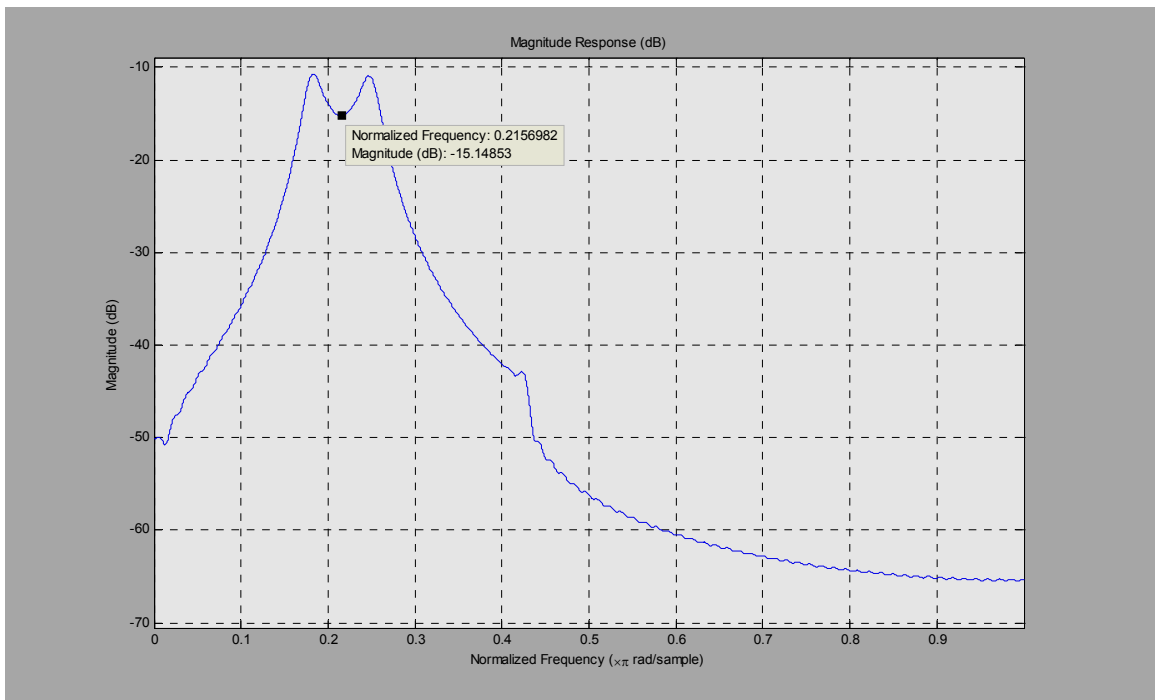analyzed individually by "fvtool" to find the normalized operating frequency.

Figure 4.2 FVTOOL Manipulation of 5-Channel Filter.

All of the manipulations take place in the filter bank function which is stored in a

variable. This final variable representation is shown in Figure 4.3. It is a digital

spectrum representation of the MEMS filter bank in the time domain. This information is

set up in the simulation function and will also be used when we set up the transmitter in

the next section. These simple manipulations to the filter bank have made it compatible

for the transmitter and receiver that we are going to simulate. This is a big step in

progressing forward as we need the results in a digital format. Now that we have what

we need, we can create the transmitter and receiver to see what our results will look like
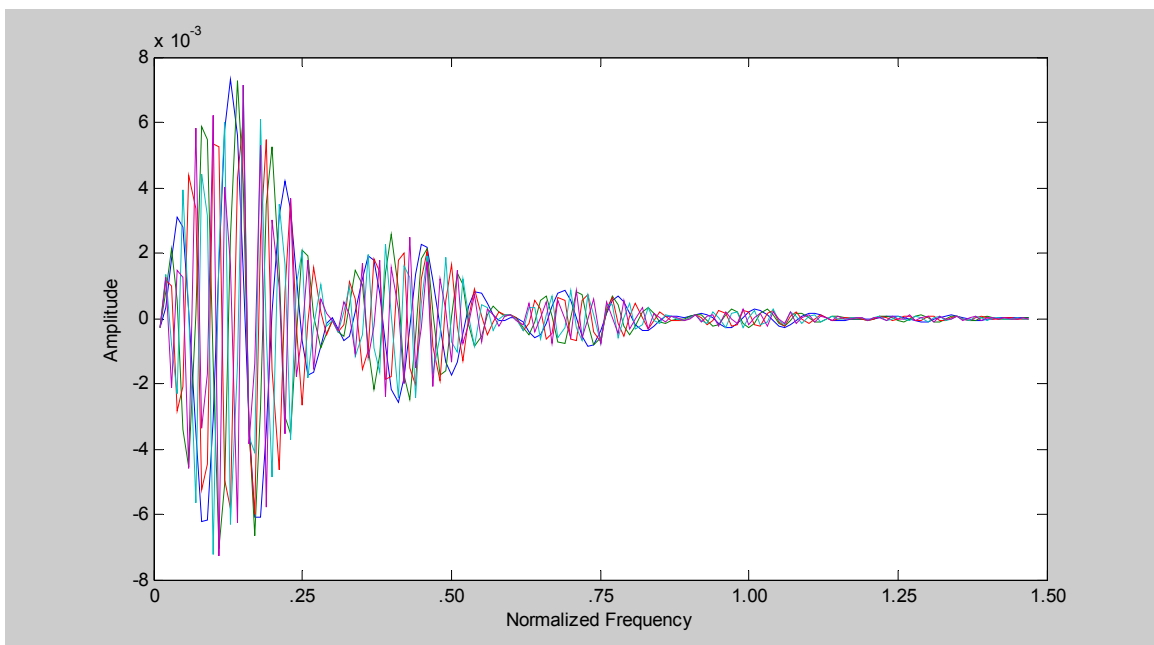
in a communications system.

Figure 4.3 Digital Spectrum of MEMS Filter.

4.2   Transmitter

Since this simulation is to test the functionality of the MEMS filter in a communication

system, a digital modulation scheme needs to be chosen. Phase Shift Keying (PSK) is a

53

digital modulation scheme that conveys data by modulating the phase of the carrier wave

where the input signal is a binary digital signal and a limited number of output phases are

possible [20]. The simplest form of PSK to test this simulation would be Binary Phase

Shift Keying (BPSK). It uses two phases which are separated by 180° and it does not

particularly matter exactly where the constellation points are positioned. A BPSK signal

can be defined by the waveform:

$$s(t) = A \cos(2\pi f_c t + m(t)) + \theta \qquad (4.4)$$

where $0 \le t \le T$, T is bit duration, A is constant, m(t) is 0° or 180° (which

represents +1 or -1), f_c is the carrier frequency, and θ is random noise. Figure 4.3 shows

the constellation diagram for BPSK systems [21]. This modulation technique is the most

reliable of all the PSK's since it takes a lot of distortion to make the demodulator reach

an incorrect decision. The downfall for this technique is it is only able to modulate at 1

bit/symbol and this makes it unsuitable for high data-rate applications when bandwidth is

limited. If a phase-shift is introduced by the communications channel or other circuitry,

the demodulator is unable to tell which constellation point is which. As a result, the data

is often differentially encoded prior to modulation [22]. This will be discussed later in
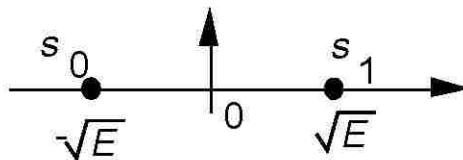
the results.

Figure 4.4 BPSK Signal Constellation.

The transmitter function is straight forward once a few things are defined. In order to set up the BPSK transmitter for this system, we need to determine certain parameters such as normalized frequencies, number of bits, sampling rate, etc. To determine the normalized frequencies, we have to use our manipulated filter bank that we previously discussed in the chapter. By looking at Figure 4.2, we can see that the center normalized frequency of this filter is 0.215. When we do that for the remaining filter banks, we get the 5 normalized frequencies that we need for the transmitter function. For completeness, the five normalized frequencies in MATLAB form are shown below:

$$[0.215 \quad 0.350 \quad 0.482 \quad 0.615 \quad 0.750] \tag{4.5}$$

The number of bits that are chosen is a user defined parameter. This number that was chosen was 1000. This appeared to be enough points to correctly simulate a signal without losing any information. In order to receive BPSK, the receiver needs to be tuned to the exact frequency of the signal. This frequency is found by setting up a ratio of the normalized frequencies to the actual frequencies. This ratio is normally:

$$1 : \frac{f_s}{2} \tag{4.6}$$

where f_s is the fixed sample frequency for the receiver. In our case, the normalized frequencies have a frequency shift difference of 1.25 MHz (each filter's center frequency is spaced 1.25 MHz apart). The normalized frequencies that we found earlier in the

chapter have a frequency shift difference of 0.133 (averages of all the ratios). When you

put this in ratio form, you get:

$$\frac{1}{0.133} = \frac{x}{1.25} \qquad (4.7)$$

where x = (f_s/2). Solving for this equation, x = 9.3785. Then solving for f_s = 18.797

MHz. The fixed frequency of the receiver should be 18.797 MHz. With this value

solved for, we're able to determine the number of samples that are needed. This is done

by solving:

$$\# \ of \ samples \ = \frac{fs}{bitrate} \qquad (4.8)$$

Our f_s is 18.797 MHz and the bitrate is 125 kHz. The bitrate can be chosen by the

user as long as you do not exceed the bandwidth of the filter. The bandwidth of the

filters is 650 kHz. So 125 kHz was chosen and that is what is used in the actual results

that will be shown later. When you run the numbers through Equation 4.8, the number of

samples that are needed is 150. This is all the information we need to set up the

transmitter.

The transmitter function is passed three variables: a random signal of 1 and -1, the

normalized frequencies, and the number of samples. It takes these three signals and

generates a BPSK signal with random noise attached. The transmitted signal is shown in

Figure 4.4. The transmitter function returns the generated signal back to the main

simulation function. As you can see, the transmitter function generated signals at the
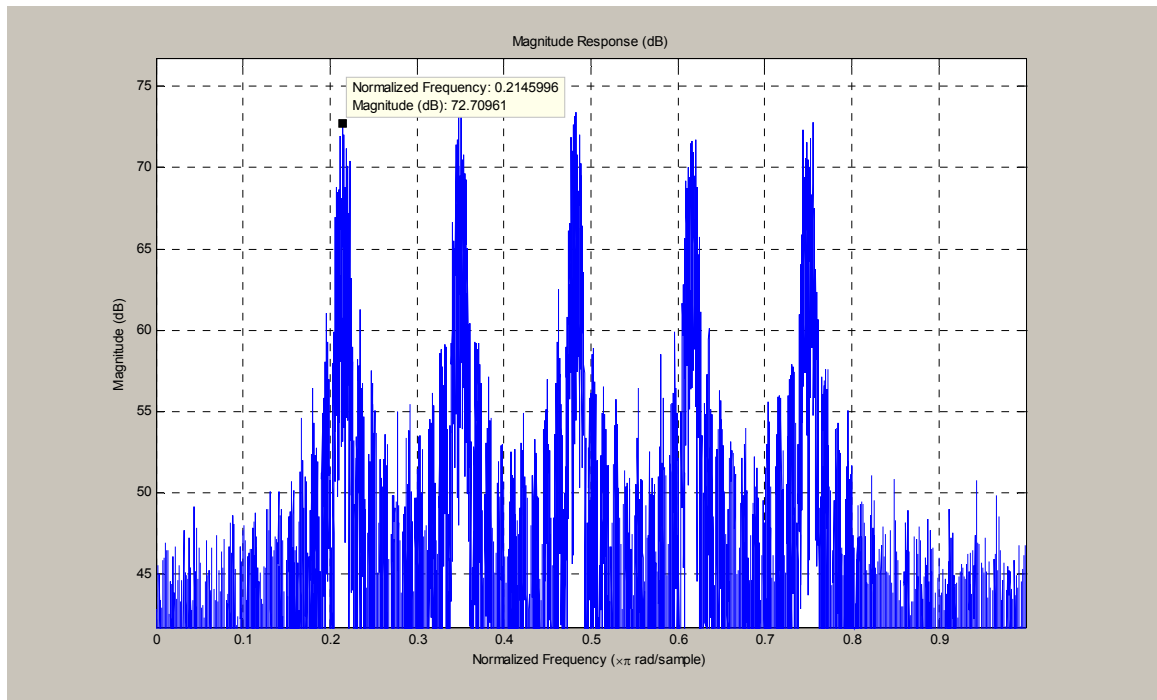
desired normalized frequencies.

Figure 4.5 The Simulated Transmitted Signal.

4.3   Receiver

The main simulation function takes the transmitted signal that we just developed and it

runs it through the 5-channel MEMS filter. The simulation also adds a gain stage to

make it more realistic. This would be similar to the front end of a receiver system. Next,

the simulation function is ready to send information to the receiver function. There are

three variables passed to the receiver function. These variables include the filtered transmitted data, the normalized frequencies, and the number of samples. The receiver then defines the in-phase and quadrature baseband signals. A low pass filter is also defined to reject all the unwanted images. Next, the data stream is mixed with the inphase and quadrature signals, and the low pass filter is applied. Essentially, the noise has been stripped out and the signal has been integrated. The decision device is coded next with the output being stored in a matrix to plot on a constellation diagram. This is the most visually attractive diagram for this case.

The simulated data from the receiver is shown in Figure 4.6. This constellation diagram shows that the BPSK signal was successfully transmitted and received. You'll notice how there are 5 different set of constellations. There are two constellations on each side of the zero plane. This is caused by intersymbol interference.
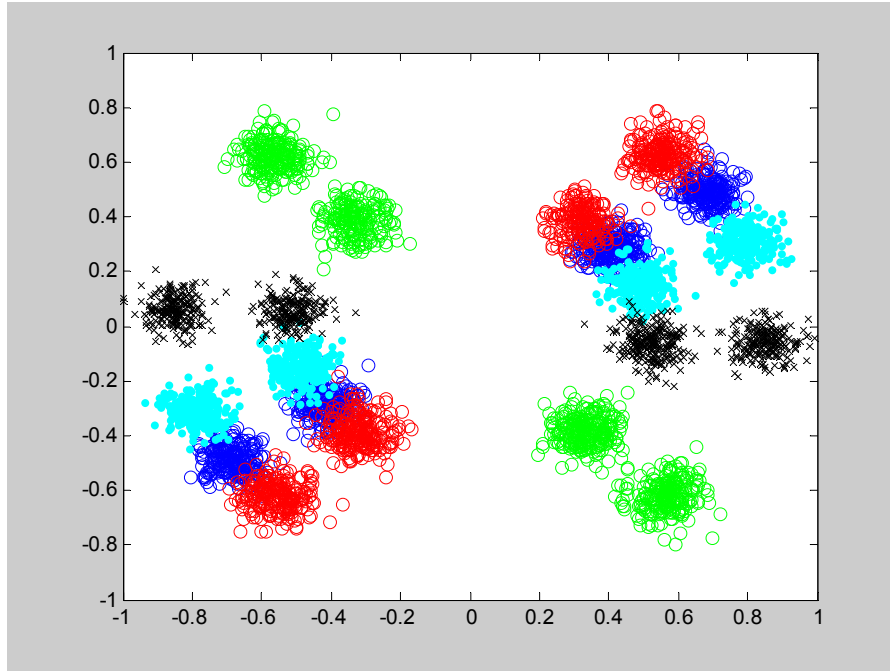
Figure 4.6 Constellation Diagram of BPSK System.

Intersymbol interference (ISI) is a form of distortion of a signal in which one symbol interferes with subsequent symbols. Usually, this is an unwanted occurrence, but in this case, it turns out to be constructive interference. Usually, ways to fight against intersymbol interference would include some type of equalization and error correcting codes. In our case, since it is constructive in the BPSK system, no action is needed, but we will show a simple method to correct the ISI later in this chapter.

Another observation that can be made from the results is the phase error. You will notice how the phase of each channel is off, except for one channel. This was expected because there is no guarantee that there would be coherence between the channels, but the challenge now is to see if we are able to correct this with some type of

circuitry or a software implementation. The circuitry that it needs to have is a Phase Locked Loop (PLL). This can also be added to the receiver to try to correct the phase error. Since this is a simulation, we will add a PLL portion to the receiver. This should correct the phase error and possibly the ISI that is created in the system.

Another analysis tool to see the results of the simulation is in the eye diagram in Figure 4.7. The eye diagram shows where the signal is repetitively sampled and applied to the vertical input, while the data rate is shown on the horizontal sweep. This is what the receiver is seeing in the baseband domain. From the results of the eye diagram, you can see that the receiver sees a reasonably square wave and there are two times at which the power is greatest. By sampling the system appropriately, we are able to maximize power. You can see the most power is not where all the transitions occur.
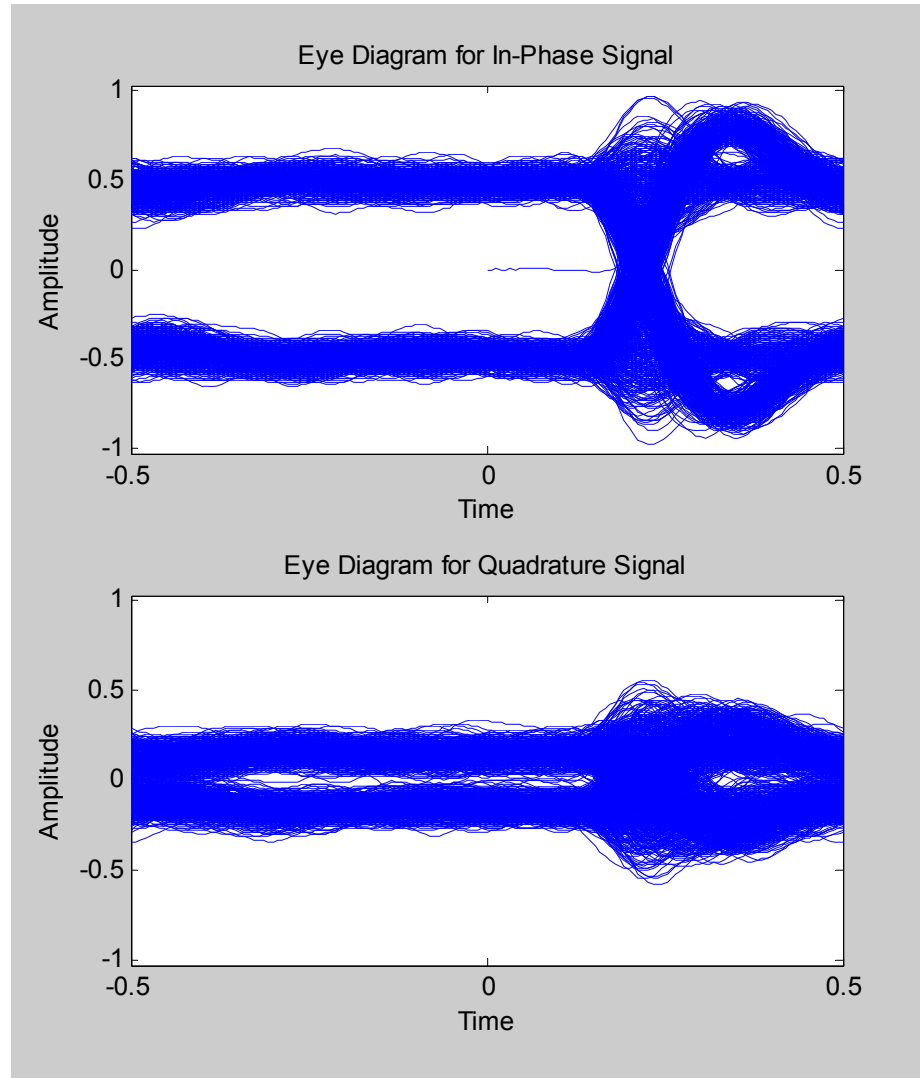
Figure 4.7 Eye Diagram of the Receiver.

After seeing these results, it was noted that a PLL must be implemented into the system. Figure 4.8 shows the results of the system with a PLL implemented. As you can see from the results, the phase error is corrected.
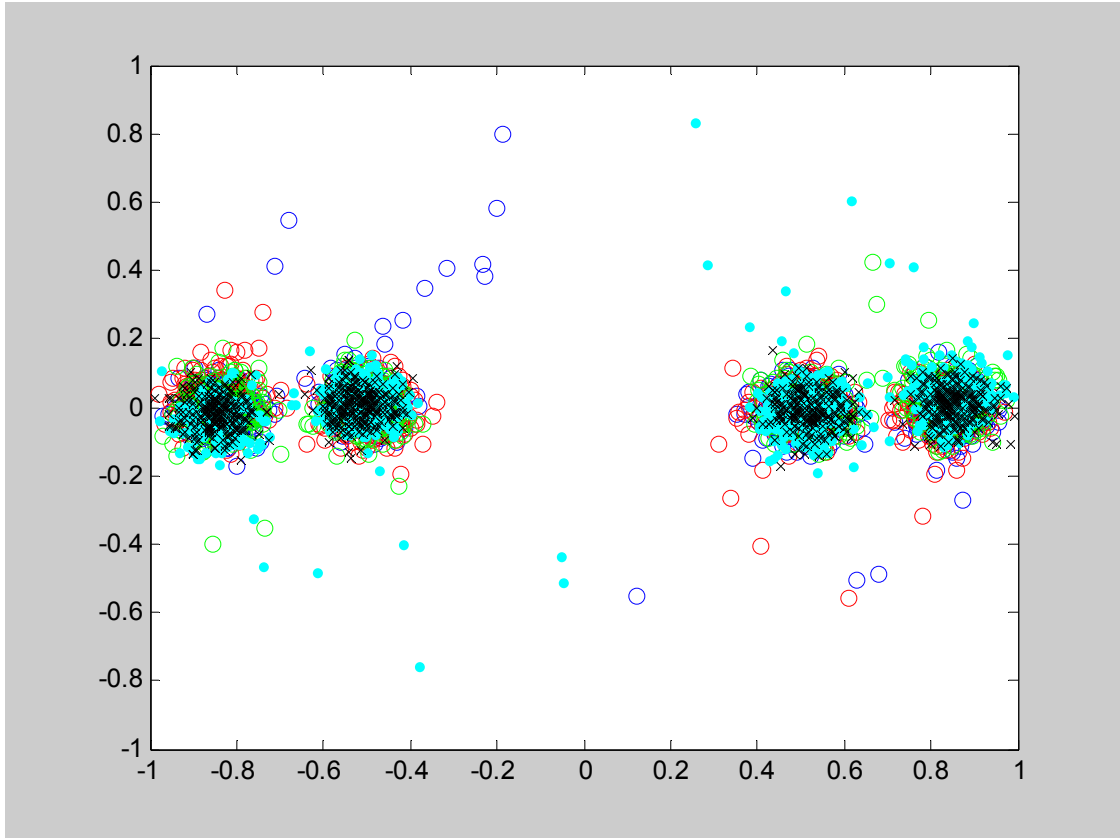
Figure 4.8 BPSK Simulation With PLL Applied.

In an effort to get rid of the multiple symbols (also known as ISI), a raised cosine filter was incorporated. The raised cosine filter is a specific electronic filter that is often used for pulse shaping in digital modulation schemes because it has the ability to minimize ISI. The raised cosine filter is an implementation of a low pass Nyquist filter and when applied properly to a digital stream, it has the property of eliminating ISI because its impulse response is zero at all nT (where n is an integer), except n = 0. Therefore, if you sample at the receiver correctly, you can completely recover the symbols that were transmitted. Ideally, a matched filter must be used in the receiver due

to white noise. The white noise creates a constraint and the way to deal with the constraint is to implement a root raised cosine filter to maintain zero ISI. In our system, MATLAB has a function called rcosfir.m. This implements a simple raised cosine filter and will suffice for our simulation purposes. The implementation of this will alleviate the ISI that is introduced by the MEMS filter and should just leave us with a BPSK constellation that is equivalent to an ideal system. Figure 4.9 shows the results of this simulation. As you can see, it has accomplished the task that we expected it to do.
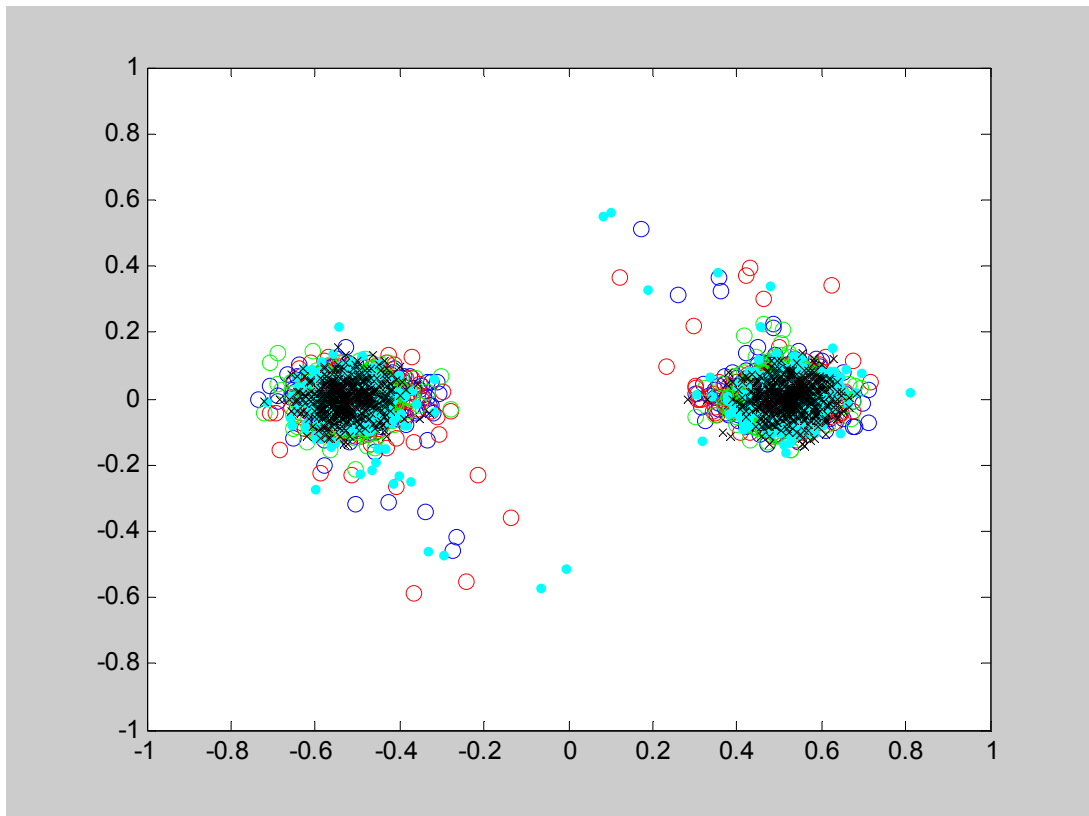

Figure 4.9 Ideal BPSK Simulation With PLL and Raised Cosine Filtering.

4.4   Actual Results

This section presents actual results for the actual 5-channel MEMS filters that were developed at Sandia National Laboratories. For this setup, a test board was built that integrated these filters with a VCO, gain stage, mixers, and other necessary circuitry. The boards have two of the filters installed on them. One filter bank is set in the corner for evaluation purposes. The other filter bank is right in the middle of the test board and that is the focus of these results. Figure 4.10 shows the layout of the 5-channel MEMS filter integrated on one chip. The size of the surface mount chip is 2.1 mm X 2.1mm.
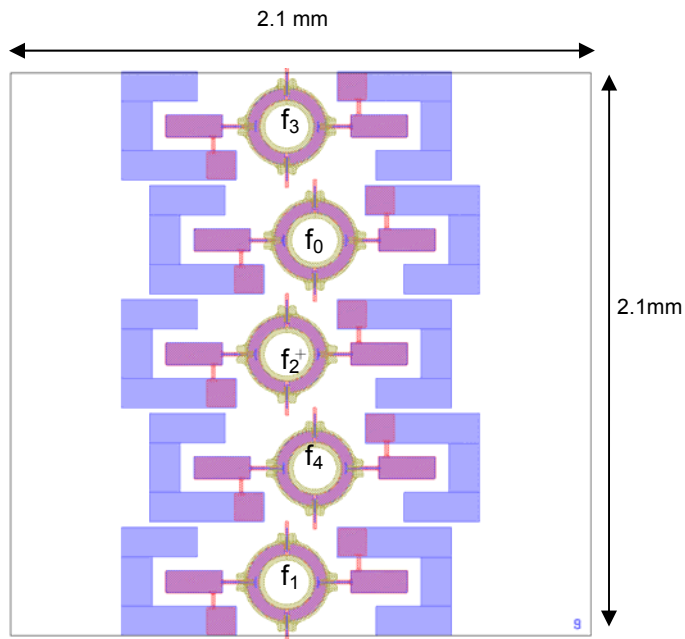

Figure 4.10 5-Channel MEMS Filter Layout.

Figure 4.11 shows a picture of the actual 5-channel MEMS filter. This filter bank that is installed on the test board has measured center frequencies of 107.77, 110.53, 111.76, and 113.32 MHz. The fifth channel (~109 MHz) is not currently working on this test board. Only two of these channels are going to be verified in the actual simulation due to the modifications that need to be implemented. This will be discussed later in the chapter.
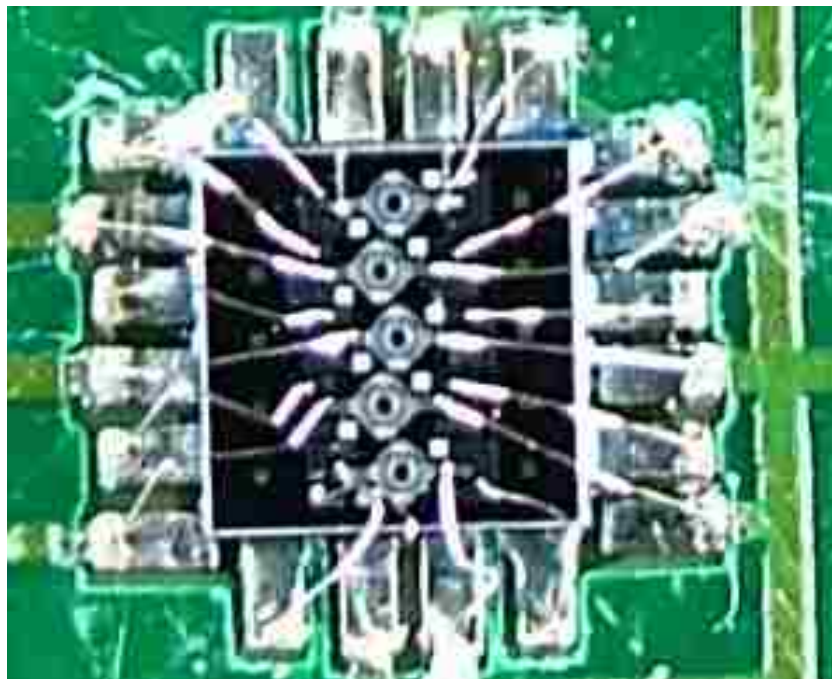

Figure 4.11 5-Channel MEMS Filter on an IC.

Figure 4.12 shows the chip with respect to some resistor circuitry around it. As you can see, the 5-channel filter bank is not much bigger than the standard surface mount

resistors. Figure 4.13 shows the test board schematic. The picture on the left is a high level schematic, while the picture on the right shows the details of the individual RX chain. Figure 4.14 shows the entire test board with all the parts. Some of the parts included are VCO's, amplifiers, mixers, potentiometers, and the basic resistors and capacitors. As you can see, the MEMS filter banks are not the limiting factor in development of the size of the board. The remaining parts are typically the same size if not bigger, making it a reality that filter banks and miniaturization is achievable. The biggest component is the VCO. All the traces on the board are 50 Ω impedances.
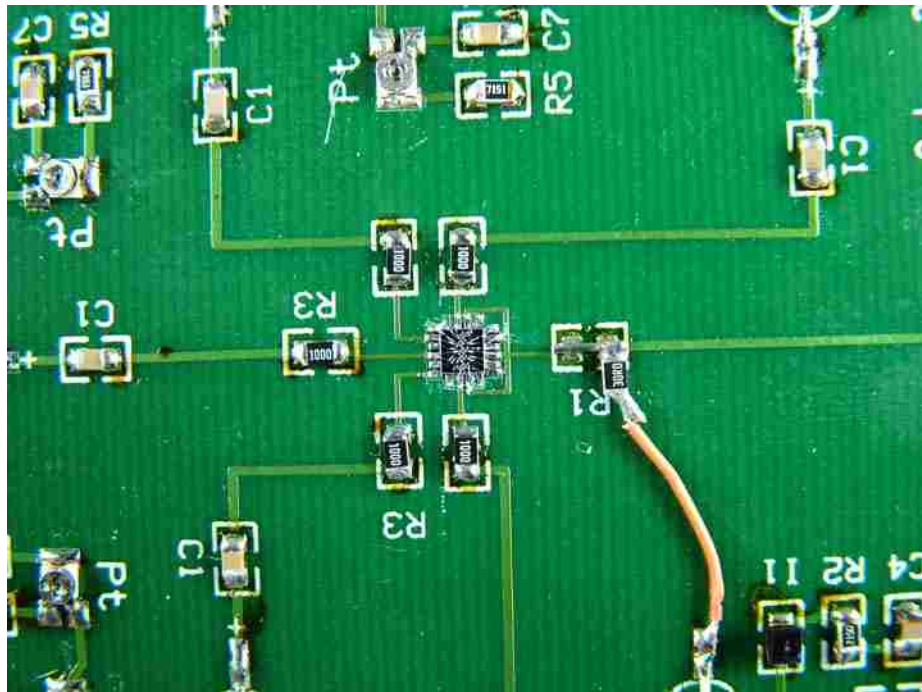

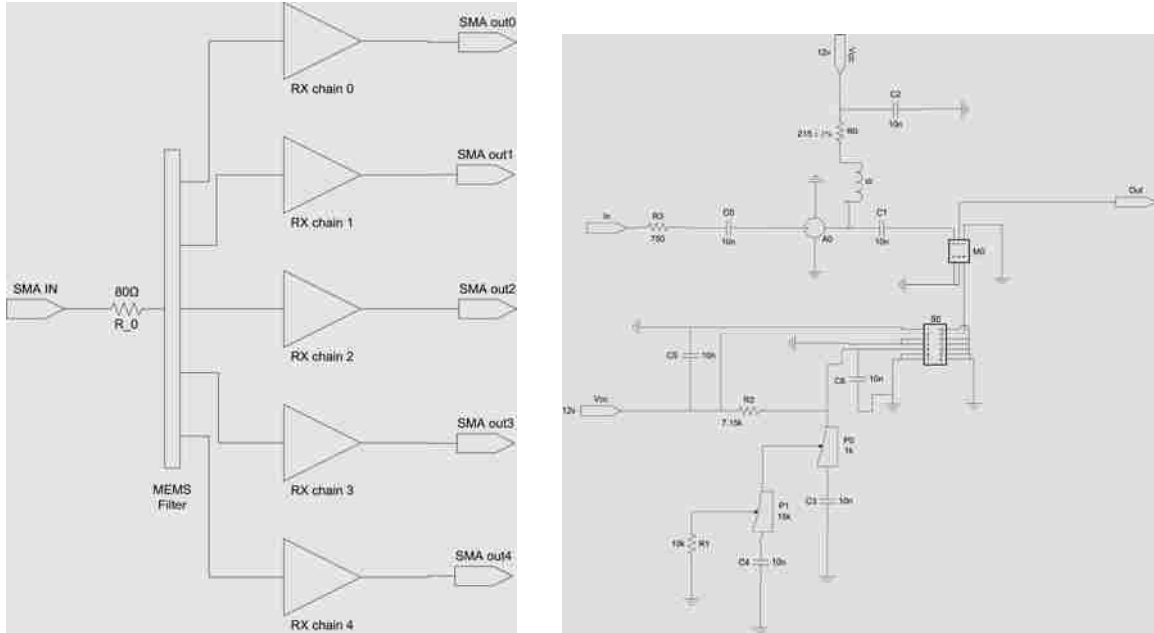Figure 4.12 Filter Bank IC With Respect toSurface Mount Resistors.

Figure 4.13 Test Board Schematic: High Level (left) Details of RX Chain (right).
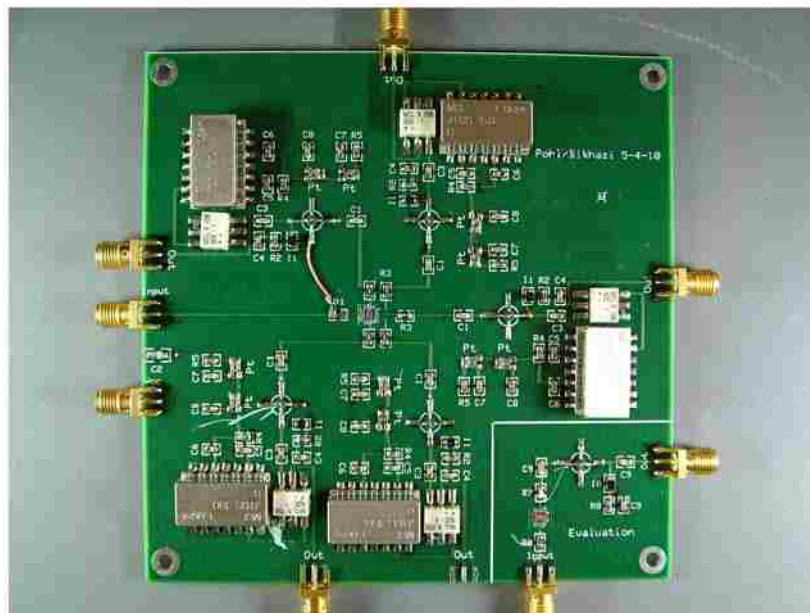

Figure 4.14 Test Board with MEMS Filters Integrated on Board.

In order to actually use the test board, a transmitter was originally going to be coded using a program called WinIQSIM and supporting hardware, such as waveform generators. WinIQSIM is specifically developed for the generation of digitally modulated signals. Complex signals can also be easily generated. It is based on a graphical user interface and is a convenient way of creating any signal that you would like to use. The signals that are generated are then sent out to a waveform generator. Due to time constraints, a transmitter was coded in VHSIC (Very High Speed Integrated Circuits) Hardware Description Language (VHDL). The VHDL transmitter was created by taking some ordinary text and converting it into a digital form like Equation 4.4. The text is just some random words that were used to create a BPSK stream. The output of the transmitter was sent to the test board and processed.

The test board takes the transmitted signal on a single input SMA. The test board is powered by 12 Volts. The input signal was originally supposed to be sent through the MEMS filter chip first. After initial testing, it was realized that the signal level needed to be amplified first. So a few haywires were installed to modify the way things were routed on the test board. This allowed the flexibility to use the same test board to amplify the signal. After the signal is amplified, it is sent through the MEMS filter. This separates and filters the signal into the five bands that we're interested in. Once processed by the MEMS filter, it is mixed down to base band. Each channel has its own VCO to aid in this process and the potentiometers are installed to manually control the

Chapter 4. BPSK Analysis

VCO voltage. The signals are then output on the OUTPUT SMA for each individual channel. The output of the board was then sent to a National Instruments (NI) Data Acquisition (DAQ) system. The NIDAQ system was chosen for its compatibility with MATLAB. The NIDAQ is able to take the incoming data from the test board and sample it appropriately (up to 2.5MS/s). The data is stored in MATLAB .mat files. These files are stored and implemented in a bpsk_dac.m file. This file is similar to the simulation file that was created for the simulation earlier in the chapter. The bpsk_dac.m file loads the .mat files and it calls the receiver function. The final thing the file does is plot the data and makes a digital movie.

The receiver function executes the same commands as previously done in the simulation. The results of the receiver function are shown in Figure 4.15 as a constellation diagram. This only shows 2 channels as the test board was not designed robustly enough to handle all 5 channels with the haywire modifications. A future test board will be fabricated to implement better engineering ideas.

The constellation diagram shown in Figure 4.15 is not a good representation of the results because it is static. For thoroughness, each point is plotted and held, but in reality, the BPSK constellation is moving.
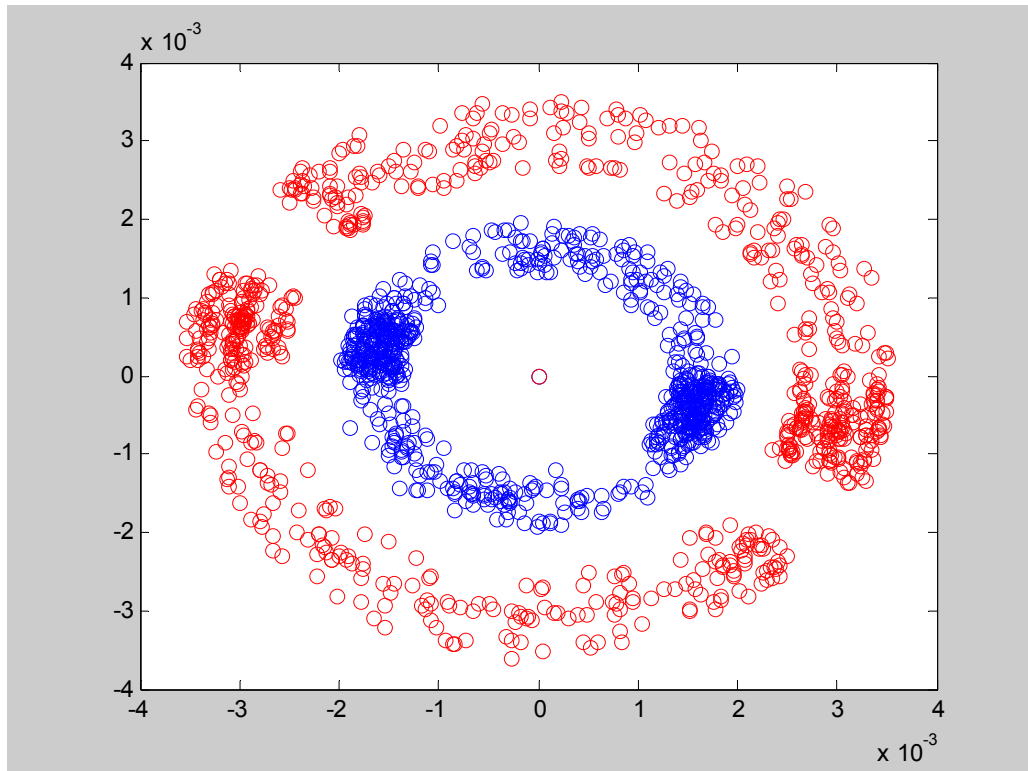
Figure 4.15 BPSK Constellation Diagram of Test Board.

The movie that was created by MATLAB shows this very well. The constellation is very interesting when you watch it in real time. The constellations start by behaving very nicely on the vertical plane and horizontal plane. We know the vertical plane is caused by phase noise as we previously determined by the simulations. The VCO is the cause of the phase noise. As the VCO frequency starts to slowly change, the phase shift of each constellation starts to "dance". It continues to do this in a clockwise and counterclockwise nature. The reason it changes direction is due to the DC resonance of the components. Essentially, the frequency of the local VCO is varying and therefore the

constellation rotates up and down as the frequency changes. The faster it rotates the faster the frequency is changing. It is a very interesting phenomenon. Figure 4.16 shows several "frames" of the movie to illustrate what is happening over time.
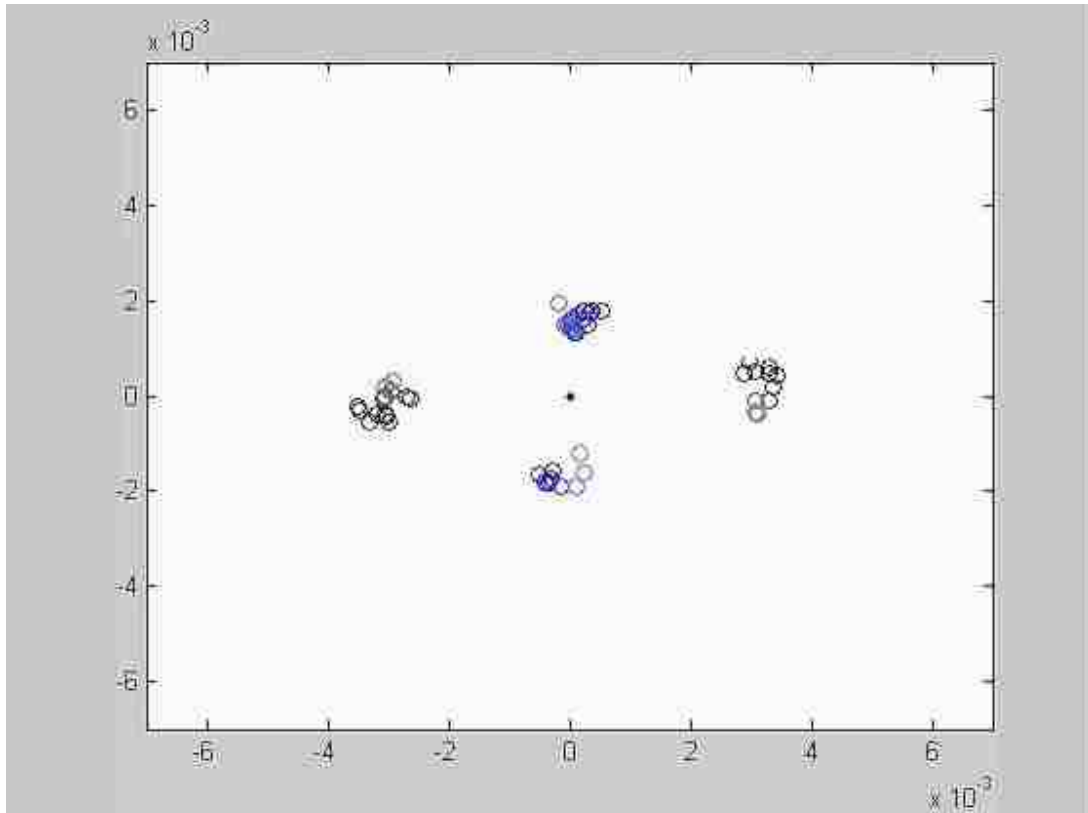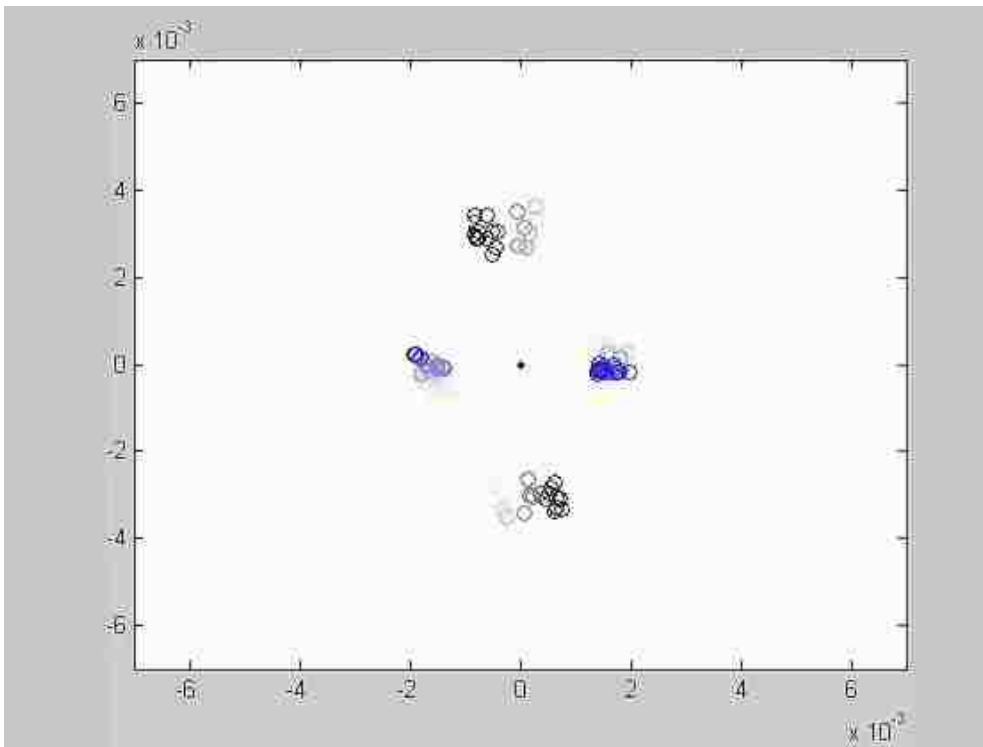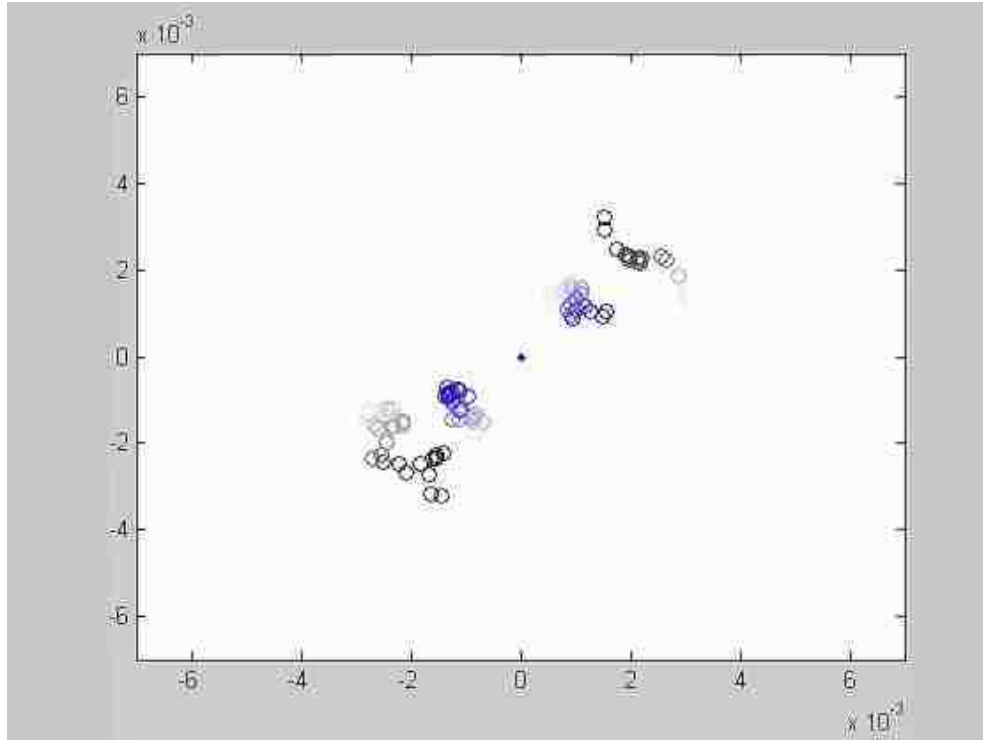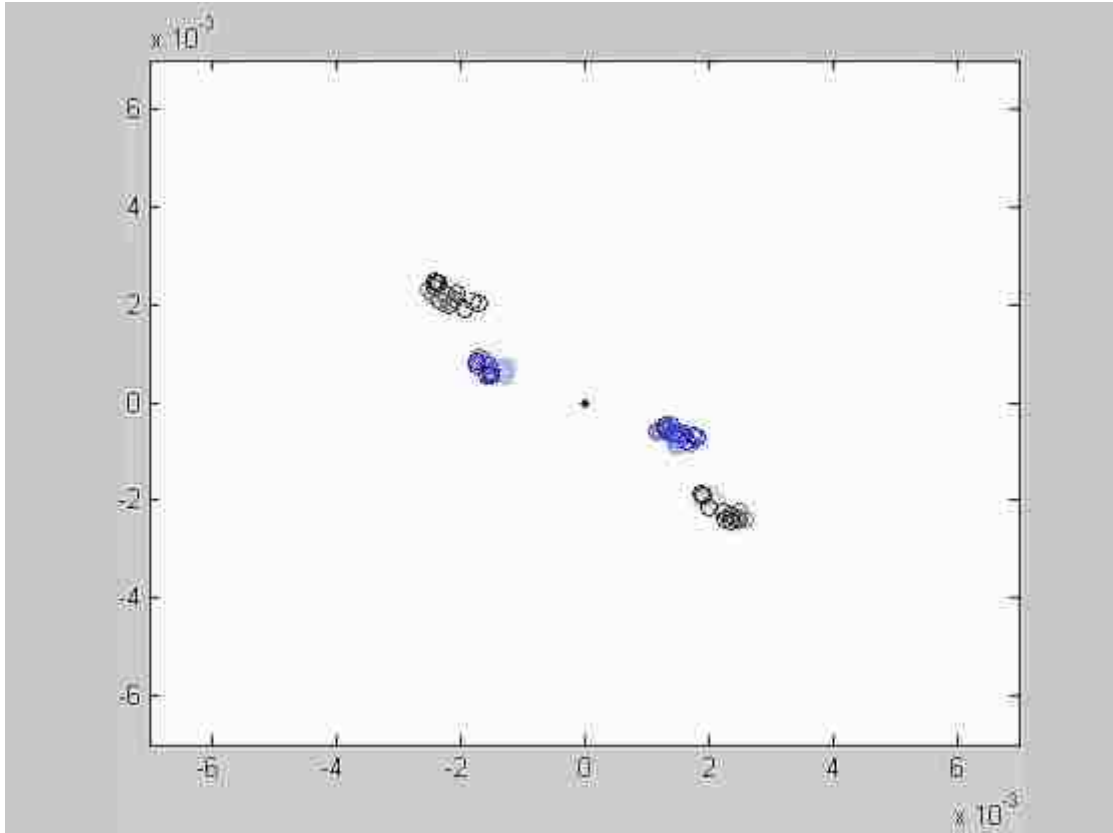
Figure 4.16 Several "Frames" With Respect to Time.

Obviously, we'd like to see if this phase shift can be corrected. So, just like the previous simulation, we will implement a PLL on the system. This PLL is implemented in the software in the receiver. The PLL circuit is used to demonstrate that even though the phase (frequency) is changing fast, a PLL can lock onto it. The PLL is able to lock on the data and keep the constellations very stable as expected. The PLL removes the phase rotation as expected, but a single PLL cannot fully correct for a frequency deviation.

Figure 4.17 shows the results of the PLL implemented on the system. Once again, the static picture does not do the results justice. The observations during real time show that the BPSK constellation does not vary much at all from the range that is shown in the figure below.
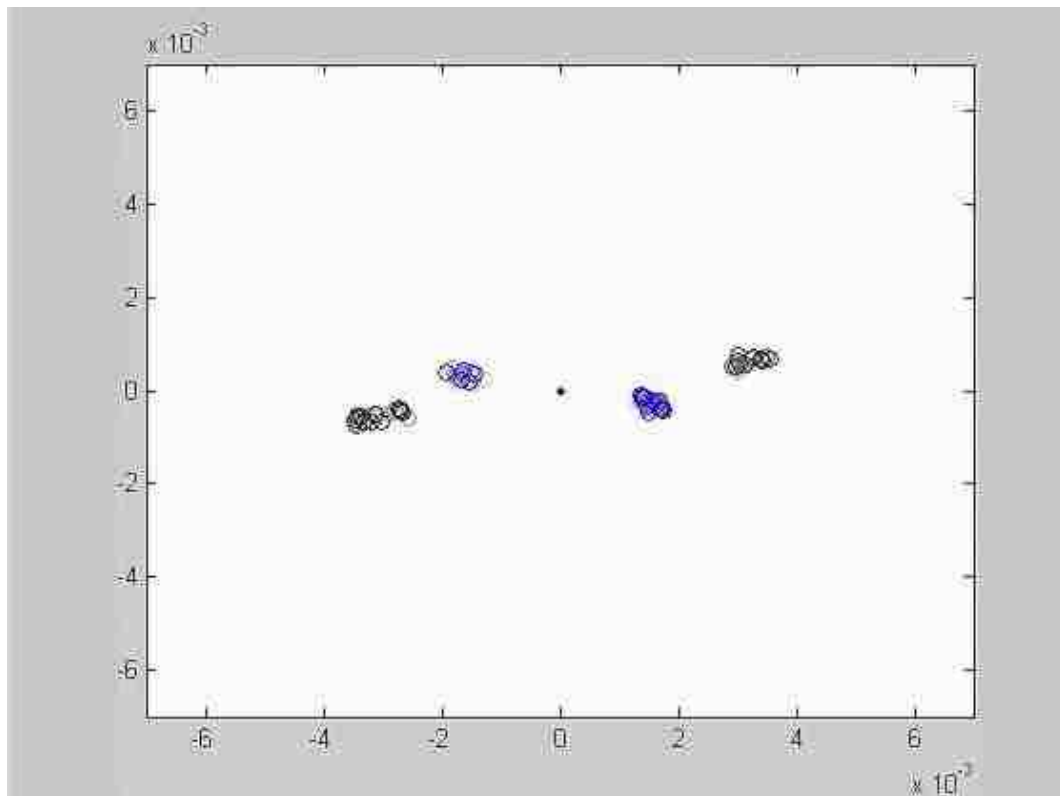

Figure 4.17 Test Board BPSK Constellation with PLL Implemented.

It is good news that the actual results resemble the simulated results. The system is functioning properly and now many more complex systems will be able to be built out of this.

4.5   Summary

This chapter extended the performance analysis presented in Chapter 3 by simulating a full BPSK system and also implementing an actual BPSK system using the MEMS 5-channel filter bank. First, baseline results were presented for the simulated system when simulating a BPSK system. Next, it was shown that the simulated systems could be validated by implementing the chips in a real circuit board. The results were as expected; however, an interesting phenomenon of intersymbol interference took place. In our case, it was constructive. The eye diagram showed how there are two places of peak power, so we are essentially stealing power in this setup. It was also noted that there was substantial phase noise. This was created in the actual setup by the VCO and in the simulations it was also present. A PLL was implemented into the receiver and this phase noise was corrected. The overall results of the simulations and test results prove that these post-CMOS compatible MEMS filters can be implemented into a full communication system.

Chapter 5

Conclusions and Future Work

This thesis first described the many RF MEMS devices that are available in industry, from switches to resonators to antennas. MEMS are redefining the micro-technology industry by making things smaller and more compatible. In Chapter 2, the various processes that are used to develop integrated circuits were introduced. These same processes have been adapted to develop the various MEMS technologies. The dual mode filter that was developed by Sandia National Laboratories was introduced for the very first time. Chapter 3 presented a performance analysis of the MEMS filters. The performance analysis showed that the MEMS filter could be simulated in MATLAB and could be verified by measuring an actual MEMS filter. This was then built into a 5-channel filter in MATLAB and that was also verified through simulation and an actual chip. This was a very important step in order to be able to use the MATLAB simulation in a BPSK system. Chapter 4 then extended the performance analysis presented in Chapter 3 by simulating a full BPSK system in MATLAB. The simulation results showed that a full BPSK system could be realized with good results. With that information, a board was designed to handle the 5-channel MEMS device. The board was tested and the results were presented. The results showed that the simulations were

correct. This information is very important because it proves that a post-CMOS 5-channel MEMS filter is achievable and will work in a system.

5.1   Future Work

Future work options that are currently taking place for continuing this analysis would be to develop a new test board to accommodate a better engineering design. The new test board would be able to test all 5 channels of the MEMS filter. Other concurrent work that is taking place for this project is experimentation with the filters. This includes further research and development of the filters to get better results. Some of the experiments that are currently taking place to further develop the filters are notching and other mechanical experiments with the design. It has been proven that physical design changes results in changes in the shape of the filters. In these experiments, the goal is to increase the frequency that the MEMS filter bank can operate at and also try to get rid of the ripple in the filter. By changing the physical characteristics of the filters, we hope we can achieve this goal. Once these steps have been accomplished and fine tuned, it is desired to implement the test board with a MEMS resonator test board into a full radio system.

When a full radio system is accomplished, there are many commercial systems that could benefit from this working system. Simulations should be done with many types of wireless communication systems. Investing in trying to increase the operating

frequency range would also help in creating better communication systems. Future simulations could include QPSK and Frequency Hopping Spread Spectrum (FHSS). There are various radio architectures that you could experiment with to implement these filters.

Not only can commercial systems benefit, but the military need would also benefit. The MEMS devices, such as resonators, have the added benefit of being smaller and so they are less prone to vibration than crystals. MEMS filters are smaller so you can pack more of them on a single die. Also, because these MEMS processes are CMOS compatible they can be built and put alongside (or on top of) typical circuit logic. Many systems in the military field could utilize unattended ground sensor applications or communication radios that talk to each other.

References

[1] **Rebeiz G., *'RF MEMS: Theory, Design and Technology'*, John Wiley and Sons,February 2003**

[2] **http://en.wikipedia.org/wiki/Microtechnology**

[3] **Allen J.J, "Micro Electro Mechanical System Design", Taylor and Francis Group, 2005**

[4] **Varadan V. K., Vinoy J. J., Jose K. A., "RF MEMS and Their Applications", John Wiley and Sons, 2002**

[5] **http://nepp.nasa.gov/index_nasa.cfm/811/**

[6] **A. R. Brown and G. M. Rebeiz, A high-performance integrated K-band diplexer, IEEE Trans. Microwave Theory Tech., Vol 47, No. 8, pp. 1477-1481, August 1999.**

[7] **http://www.eecs.umich.edu/rebeiz/Current_VII_Press.html**

[8] **R. C. Ruby, A. Barfknecht, C. Han, Y. Desai, F. Geefay, G. Gan, M. Gat, and T. Verhoeven, "High-Q FBAR filters in a wafer-level chip-scale package", in IEEE International Solid-State Circuits Conference Digest, 2002, pp. 184-458.**

[9] **J. McDonald, "Electronic Products", *MEMS oscillators 101,* November 2007.**

[10] **J.R. Clark, M. Pai, B. Wissman, G. He, and W.-T. Hsu, "Parallel-Coupled Square-Resonator Micromechanical Filter Arrays", International Frequency Control Symposium and Exposition, IEEE, June 2006, pp. 485-490**

[11] **D. Forman, Automotive applications, *smalltimes*, 3(3), 42-43, May/June 2003.**

[12] **W.M. Middleton, M.E. Van Valkenburg, "Reference Data for Engineers: Radio, Electronics, Computer, and Communications" Newnes, 2002.**

References

[13] H. Helvajian, M. Mehregany, S. Roy "Microengineering Aerospace Systems", AIAA, Aerospace Press Series, 1999.

[14] K. J. Smart, R. H. Olsson III, D. Ho, D. R. Heine, and J. G. Fleming, "Frequency agile radios using MEMS resonators," *Proc. of the Govt. Microcircuit App. and Critical Tech. Conf.*, pp. 409-412, March 2007.

[15] G. Piazza, P.J. Stephanou, J.P. Black, R.M. White and A. P. Pisano, "Single-Chip Multiple-Frequency RF Microresonators based on Contour-Mode and FBAR Technologies," *2005 IEEE Ultrasonic Symposium,* Rotterdam, pp. 1187 - 1190, 2005.

[16] Roy H. Olsson III, James G. Fleming, Kenneth E. Wojciechowski, Michael S. Baker, and Melanie R. Tuck, "Post-CMOS Compatible Aluminum Nitride MEMS Filters and Resonant Sensors" Frequency Control Symposium, 2007 Joint with the 21st European Frequency and Time Forum. IEEE International, pp. 412-419, May 29 2007-June 1 2007.

[17] P. J. Stephanou, G. Piazza, C. D. White, M. B. J. Wijesundara, and A. P. Pisano, "Piezoelectric thin film AlN annular dual contour mode bandpass filter," *Proc. ASME IMECE2005,* 2005.

[18] E. Cheever, http://www.swarthmore.edu/NatSci/echeeve1/Ref/mna/MNA2.html

[19] A.V. Oppenheim, A.S. Willsky, S.H. Nawab, "Signals and Systems," Prentice Hall, Upper Saddle River, New Jersey 07458, 1997, 2nd Edition.

[20] W. Tomasi, "Electronic Communication Systems Fundamentals Through Advanced" , Prentice Hall Upper Saddle River, New Jersey 07458, 2001, 4th Edition.

[21] M. Schwartz, Information Transmission, Modulation, and Noise, 4/e, McGraw Hill, 1990.

[22] J.G. Proakis, "Digital Communications", McGraw-Hill 1221 Avenue of the Americas New York, NY 10020, August 2000, 4th Edition.